

Supporting Information (SI)

Mbandakamines A and B, Unsymmetrically Coupled Dimeric Naphthylisoquinoline Alkaloids, from a Congolese *Ancistrocladus* Species

**Gerhard Bringmann,^{†,*} Blaise Kimbadi Lombe,^{†,‡} Claudia Steinert,[†] Karine Ndjoko Ioset,[†]
Reto Brun,^{§,II} Florian Turini,[#] Günther Heubl,[#] and Virima Mudogo[‡]**

Institute of Organic Chemistry, University of Würzburg, Am Hubland, D-97074 Würzburg, Germany, Faculté des Sciences, Université de Kinshasa, B.P. 202, Kinshasa XI, Democratic Republic of the Congo, Swiss Tropical and Public Health Institute, Socinstrasse 57, CH-4002 Basel, Switzerland, University of Basel, Petersplatz 1, CH-4003 Basel, Switzerland, and Department of Biology I, Biodiversity Research, Section Systematic Botany, Ludwig-Maximilians University Munich, Menzinger Straße 67, D-80638 München, Germany

**To whom correspondence should be addressed: Fax: +49-931-3184755; Tel: +49-931-3185323. Email: bringman@chemie.uni-wuerzburg.de*

Table of Contents	Page
Experimental Section	1-7
Figure S1. Genotype frequencies of <i>Ancistrocladus</i> in the Mbandaka region	8
Table S2. ^1H , ^{13}C , HMBC, and ROESY NMR spectral data of mbandakamine A (1)	9-10
Table S3. ^1H , ^{13}C , HMBC, and ROESY NMR spectral data of mbandakamine B (2)	11-12
Figures S4a-c. ^1H NMR spectra of compound 1 in methanol- d_4	13-15
Figures S5a-c. ^{13}C NMR spectra of compound 1 in methanol- d_4	16-18
Figures S6a-c. DEPT NMR spectra of compound 1 in methanol- d_4	19-21
Figures S7a-c. COSY spectra of compound 1 in methanol- d_4	22-24
Figures S8a-c. ROESY spectra of compound 1 in methanol- d_4	25-27
Figures S9a-c. HSQC spectra of compound 1 in methanol- d_4	28-30
Figures S10a-c. HMBC spectra of compound 1 in methanol- d_4	31-33
Figure S11. HRESIMS spectrum of compound 1	34
Figure S12. IR spectrum of compound 1	35
Figure S13. CD spectrum of compound 1	36
Figure S14. Oxidative degradation products of compound 1	37
Figures S15a-c. ^1H NMR spectra of compound 2 in methanol- d_4	38-40
Figures S16a-c. ^{13}C NMR spectra of compound 2 in methanol- d_4	41-43
Figures S17a-c. DEPT NMR spectra of compound 2 in methanol- d_4	44-46
Figures S18a-c. COSY spectra of compound 2 in methanol- d_4	47-49
Figures S19a-c. ROESY spectra of compound 2 in methanol- d_4	50-52

Figures S20a-c. HSQC spectra of compound 2 in methanol- d_4	53-55
Figures S21a-c. HMBC spectra of compound 2 in methanol- d_4	56-58
Figure S22. HRESIMS spectrum of compound 2	59
Figure S23. IR spectrum of compound 2	60
Figure S24. CD spectrum of compound 2	61
Figure S25. Oxidative degradation products of compound 2	62

Experimental Section

General Experimental Procedures

UV/Vis spectra were taken on a Cary 50 Conc spectrophotometer (Varian), IR spectra on a JASCO FT-IR-410 spectrometer, and optical rotations on a JASCO P-1020 polarimeter. The CD spectra were recorded on a J-715 spectropolarimeter (JASCO) at room temperature using a 0.02-cm standard cell and spectrophotometric-grade MeOH, and are reported in $\Delta\epsilon$ values [$\text{cm}^2\text{mol}^{-1}$] at the given wavelength λ [nm]. ^1H NMR and ^{13}C NMR spectra were measured on a DMX 600 (600 MHz) instrument. Chemical shifts (δ) are reported in parts per million (ppm) with the proton of carbon-13 signals of methanol (^1H , $\delta = 3.31$ ppm; ^{13}C , $\delta = 49.15$ ppm) in the deuterated solvent as internal reference. HRESIMS spectra were obtained on a microTOF-focus mass spectrometer (Bruker). Preparative HPLC was performed on a JASCO HPLC system (PU-2087, UV-2077, LC-NetII/ADC), using a SymmetryPrep C18 column (Waters, 19 x 300 mm, 7 μm) and a Chromolith SemiPrep RP-18e column (100 x 10 mm), with the UV absorption wavelengths set at 232, 254, and 310 nm. Organic solvents were analytical grade or distilled prior to use.

Plant Material

The *Ancistrocladus* plant material was collected in the vicinity of the town of Mbandaka in the province of Equateur in the Democratic Republic of Congo, in August 2008 (GPS coordinates 00°06.191S, 018°20.506E). A voucher specimen (No. 032) has been deposited at the Herbarium Bringmann, University of Würzburg.

Extraction and Isolation

Air-dried and powdered leaves (400 g) were exhaustively extracted with an acidified CH_2Cl_2 -EtOH mixture (1:1, v/v; 200 mL of solvent mixture + 15 mL of conc. HCl). After neutralization with sodium hydroxide the suspension was filtered and the solvent was evaporated under reduced pressure. The solid crude extract was macerated in chloroform and the remaining residue (3.6 g of alkaloidic fraction) was dissolved in methanol. By preparative HPLC on a SymmetryPrep C18 column with a flow rate of 1 mL/min from 0 to 1 min and 8 mL/min from 1 to 40 min and a solvent system consisting of (A) H_2O (+ 0.05% TFA) and (B) MeOH (+ 0.05%

TFA), the plant extract was resolved to give 13 fractions. For separation the following gradient system was employed: 0 min 18% B, 35.5 min 33% B, 36-38 min 100% B, 38.5 min 18% B.

Fraction 5 (t_R = 27.1 min; containing **1**) was further purified by chromatography on a Chromolith SemiPrep RP-18e column (100 x 10 mm) using a gradient solvent system consisting of (A) H₂O / MeOH 9:1 (+ 0.05% TFA) and (B) H₂O / MeOH 1:9 (+ 0.05% TFA): 0 min 0% B, 7 min 25% B, 7.5-8.5 min 100% B, 9 min 0% B and the flow rate 10 mL/min, to yield 13 mg of **1**.

Fraction 11 (t_R = 33.8 min; containing **2**) was further purified by chromatography on a Chromolith SemiPrep RP-18e column (100 x 10 mm) using a gradient solvent system consisting of (A) H₂O / ACN 9:1 (+ 0.05% TFA) and (B) H₂O / ACN 1:9 (+ 0.05% TFA): 0 min 15% B, 7 min 25% B, 7.5-8.8 min 100% B, 9.2 min 15% B and the flow rate 8 mL/min, to yield 3.5 mg of **2**.

Mbandakamine A (**1**)

Colorless solid; m.p. > 360 °C; $[\alpha_D^{20}]$ +38 (MeOH; c 0.01); UV (MeOH): λ_{\max} (log ϵ) nm: 348 (3.7), 332 (3.8), 318 (3.8), 290 (3.7), 230 (4.4); CD cm²mol⁻¹: $\Delta\epsilon_{319}$ +4, $\Delta\epsilon_{290}$ -3.6, $\Delta\epsilon_{248}$ +7, $\Delta\epsilon_{230}$ -30, $\Delta\epsilon_{200}$ +32 (MeOH; c 0.1); IR (ATM): ν_{\max} cm⁻¹: 3140, 3047, 2848, 2360, 2336, 1595, 1406, 1108, 1077, 667, 619; ¹H and ¹³C NMR data: see Table S1; HRESIMS: m/z : 785.37980 [M+H]⁺ (calcd for C₄₈H₅₃N₂O₈⁺ 785.37964).

Mbandakamine B (**2**)

Colorless solid; m.p. > 360 °C; $[\alpha_D^{20}]$ -38 (MeOH; c 0.01); UV (MeOH): λ_{\max} (log ϵ) nm: 345 (3.4), 330 (3.5), 319 (3.5), 293 (3.4), 230 (4.2); CD cm²mol⁻¹: $\Delta\epsilon_{348}$ -0.9, $\Delta\epsilon_{311}$ -1.1, $\Delta\epsilon_{269}$ +1.7, $\Delta\epsilon_{244}$ -3.6, $\Delta\epsilon_{221}$ +6, $\Delta\epsilon_{206}$ -4, (MeOH; c 0.1); IR (ATM): ν_{\max} cm⁻¹: 2924, 2852, 2360, 2336, 1677, 1204, 1137, 1054, 841, 803, 670; ¹H and ¹³C NMR data: see Table S2; HRESIMS: m/z : 785.37899 [M+H]⁺ (calcd for C₄₈H₅₃N₂O₈⁺ 785.37964).

Oxidative Degradation

Ruthenium(III)-catalyzed periodate degradation, derivatization of the resulting amino acids with MeOH/HCl and then with (*R*)- α -methoxy- α -trifluoromethylphenylacetyl chloride [(*R*)-MTPA-Cl, prepared from (*S*)-MTPA], and subsequent GC-MSD analysis were carried out as described earlier.[1,2]

Biological Experiments

Antiparasitic activities against the pathogens *Plasmodium falciparum* (NF54 strain), *Trypanosoma cruzi*, *Trypanosoma brucei rhodesiense*, and *Leishmania donovani* (all tested in Basel) and the cytotoxicity against mammalian host cells (rat skeletal myoblast L6 cells) were assessed as described by some of us.[3]

[1] Bringmann, G.; Geuder, T.; Rübenacker, M.; Zagst, R. *Phytochemistry* **1991**, *30*, 2067–2070.

[2] Bringmann, G.; God, R.; Schäffer, M. *Phytochemistry* **1996**, *43*, 1393–1403.

[3] Orhan, I.; Sener, B.; Kaiser, M.; Brun, R.; Tasdemir, D. *Mar. Drugs* **2010**, *8*, 47–58.

Population Genetic Analysis

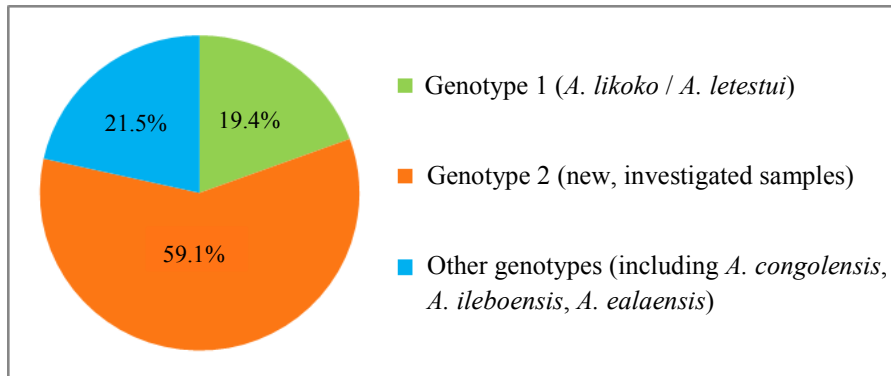
Multilocus microsatellite fingerprint data of 82 *Ancistrocladus* individuals from twelve collection sites in the Democratic Republic of Congo were retrieved (unpublished) and subjected to a population structure analysis using Structure 2.3.4 [1], applying standard analysis parameters. The most likely number of genetic clusters was inferred using the method of Evanno *et al.* [2], as implemented in Structure Harvester [3]. For the present study, information was inferred from a population subset with focus on the samples under investigation. Further results will be presented in an extensive future study.

[1] Earl, D.A.; von Holdt, B. M. *Conserv. Genet. Resour.* **2012**, *4*, 359-361.

[2] Evanno, G.; Regnaut, S.; Goudet, J. *Mol. Ecol.* **2005**, *14*, 2611-2620.

[3] Pritchard, J. K.; Stephens, M.; Donnelly, P. *Genetics* **2000**, *155*, 945-959.

Figure S1. Genotype frequencies at the Mbandaka collection area as inferred by a population structure analysis.



A genetic structure analysis of several Congolese *Ancistrocladus* populations based on microsatellite fingerprint data indicated the presence of several different genotypes (Figure S1) at the collection sites in the tropical rain forest near the town Mbandaka. The samples used for the present study belong to the most frequent genetic cluster, which occurs exclusively in the Mbandaka region and is not associated with any yet botanically described species. Further investigation will be performed on morphological and chemical evidence that could confirm the demarcation of this genetic fingerprint. A survey of observable differences across distinct genetic clusters within populations, and of detectable similarities across genetic clusters that are represented in different populations might render the description of a new species possible.

Table S2. ^1H , ^{13}C , HMBC, and ROESY NMR spectroscopic data of **1** in MeOD.^{a,b}

Position	^1H	^{13}C	HMBC (H \rightarrow C)	ROESY
1	4.79 (<i>q</i> , 6.7)	49.4	3, 8, 9, 1-CH ₃	1-CH ₃ , 8-OCH ₃
3	3.70 (<i>m</i>)	45.6	3-CH ₃	4 _{eq} , 1-CH ₃ , 3-CH ₃
4 _{ax}	2.52 (<i>dd</i> , 18.0, 11.7)	32.9	3, 9, 10, 3-CH ₃	3, 4 _{eq} , 1', 7''' , 3-CH ₃ , 8'''-OCH₃
4 _{eq}	3.89 (<i>dd</i> , 18.1, 4.5)	32.9	5, 9, 10	3, 4 _{ax} , 7''' , 3-CH ₃
5		120.5		
6		157.6		
7	6.46 (<i>s</i>)	98.5	1, 5, 6, 8, 9	8-OCH ₃
8		157.3		
9		113.1		
10		133.6		
1'	6.62 (<i>pt</i> , 1.2)	118.8	3', 4', 8', 9', 10', 2'-CH ₃	4 _{ax} , 2'-CH ₃ , 8'''-OCH₃
2'		136.4		
3'	6.74 (<i>d</i> , 1.2)	106.9	1', 2', 4', 9', 2'-CH ₃	2'-CH ₃ , 4'-OCH ₃ , 8'''-OCH₃
4'		157.4		
5'		151.0		
6'		124.1		
7'	6.44 (<i>s</i>)	134.4		4 _{eq} , 2''-CH ₃
8'		124.3		
9'		135.9		
10'		114.4		
1''		127.8		
2''		140.9		
3''	6.78 (<i>s</i>)	114.5	1'', 4'', 10'', 2''-CH ₃	2''-CH ₃
4''		155.3		
5''		158.4		

6"	7.00 (<i>d</i> , 7.9)	104.7	5", 8", 10"	5"-OCH ₃ , 7"
7"	7.05 (<i>d</i> , 7.9)	132.2	5", 9", 5'''	6", 4''' _{eq}
8"		126.3		
9"		138.1		
10"		116.2		
1'''	4.64 (<i>q</i> , 6.7)	49.9	3''', 8''', 9''', 1'''-CH ₃	4'-OCH₃ , 1'''-CH ₃ , 8'''-OCH ₃
3'''	3.5 (<i>m</i>)	46.1		4''' _{eq} , 1'''-CH ₃ , 3'''-CH ₃
4''' _{ax}	2.42 (<i>dd</i> , 18.0, 11.7)	33.1	3''', 5''', 9''', 10''', 3'''-CH ₃	3''', 4''' _{eq} , 3'''-CH ₃
4''' _{eq}	1.97 (<i>dd</i> , 18.0, 4.3)	33.1	5''', 9''', 10'''	7'', 3'', 4''' _{ax} , 3'''-CH ₃
5'''		122.7		
6'''		154.3		
7'''	5.32 (<i>s</i>)	96.8	8'', 5''', 6''', 8''', 9'''	4_{ax} , 3-CH₃ , 8-OCH₃ , 8'''-OCH ₃
8'''		156.5		
9'''		113.4		
10'''		133.5		
1-CH ₃	1.57 (<i>d</i> , 6.7)	18.7	1	1, 3, 8-OCH ₃
3-CH ₃	1.49 (<i>d</i> , 6.5)	19.6	3, 4	3, 4 _{ax} , 4 _{eq} , 7''' , 8'''-OCH₃
8-OCH ₃	3.85 (<i>s</i>)	55.9	8	1, 7, 1-CH ₃
2'-CH ₃	2.34 (<i>s</i>)	22.0	1', 2', 3', 9', 10'	1', 3', 8'''-OCH₃
4'-OCH ₃	4.09 (<i>s</i>)	56.7	4'	3', 1''', 8'''-OCH₃
2''-CH ₃	1.88 (<i>s</i>)	21.3	6', 1'', 2'', 3'', 8'', 9''	7', 3''
5''-OCH ₃	4.15 (<i>s</i>)	56.8	5''	6'', 7''
1'''-CH ₃	1.53 (<i>d</i> , 6.7)	18.8	1'''	1''', 3''', 8'''-OCH ₃
3'''-CH ₃	1.25 (<i>d</i> , 6.5)	18.7	3''', 4'''	3''', 4''' _{ax} , 4''' _{eq}
8'''-OCH ₃	3.03 (<i>s</i>)	55.3	8'''	4_{ax} , 1' , 3' , 1''', 7''', 3-CH₃ , 2'-CH₃ , 4'-OCH₃ , 1'''-CH ₃

[a] Multiplicities and coupling constants *J* [Hz] are shown in parentheses, δ values are given in ppm.

[b] ROESY correlations between **1a** and **1b** are marked in bold.

Table S3. ^1H , ^{13}C , HMBC, and ROESY NMR spectroscopic data of **2** in MeOD.^{a,b}

Position	^1H	^{13}C	HMBC ($\text{H} \rightarrow \text{C}$)	ROESY
1	4.73 (<i>q</i> , 6.8)	49.01	3, 8, 9, 10, 1-Me	1-CH ₃ , 8-OCH ₃
3	3.65 (<i>m</i>)	44.71		4 _{eq} , 1-CH ₃ , 3-CH ₃
4 _{ax}	1.72 (<i>dd</i> , 18.1, 11.7)	33.23	3, 10, 3-Me	4 _{eq} , 3-CH ₃
4 _{eq}	2.65 (<i>dd</i> , 18.1, 4.9)	33.23	5, 9, 10	3, 4 _{ax} , 7', 3-CH ₃ , 2''-CH₃
5		120.20		
6		155.91		
7	6.71 (<i>s</i>)	98.83	5, 6, 8, 9	8-OCH ₃
8		157.61		
9		115.36		
10		133.96		
1'	6.51 (<i>pt</i> , 0.9)	118.59	3', 8', 10', 2'-Me	2'-CH ₃
2'		139.57		
3'	6.77 (<i>d</i> , 0.9)	107.78	1', 4', 10', 2'-Me	2'-CH ₃ , 4'-OCH ₃ , 8'''-OCH₃
4'		158.01		
5'		153.17		
6'		136.13		
7'	6.86 (<i>s</i>)	133.26	5, 5', 6', 6''	4 _{eq} , 2''-CH ₃ , 4'''_{ax}
8'		122.89		
9'		137.16		
10'		115.05		
1''		126.65		
2''		139.56		
3''	6.85 (<i>s</i>)	114.73	1'', 4'', 5'', 9'', 2''-Me	2''-CH ₃
4''		155.61		
5''		158.13		

6"	7.01 (<i>d</i> , 8.1)	104.89	4'', 8'', 9'', 10''	5"-OCH ₃
7"	6.98 (<i>d</i> , 8.1)	132.69	8'', 9'', 10'', 4''' _{eq} , 5'''	5"-OCH ₃ , 4''' _{eq}
8"		127.38		
9"		137.43		
10"		116.16		
1'''	4.38 (<i>q</i> , 6.8)	49.33	3''', 8''', 9''', 10''', 1'''-Me	1'''-CH ₃ , 8'''-OCH ₃
3'''	3.42 (<i>m</i>)	45.42	1'''	4''' _{eq} , 1'''-CH ₃ , 3'''-CH ₃
4''' _{ax}	1.96 (<i>dd</i> , 18.2, 10.9)	33.62	3''', 10'''	4''' _{eq} , 7', 3'''-CH ₃
4''' _{eq}	2.22 (<i>dd</i> , 18.2, 4.1)	33.62	5''', 9''', 10'''	7'', 4''' _{ax}
5'''		123.69		
6'''		156.22		
7'''	5.94 (<i>s</i>)	98.70	8'', 5''', 6''', 9'', 10'''	4'-OCH₃ , 8'''-OCH ₃
8'''		156.31		
9'''		113.08		
10'''		131.17		
1-CH ₃	1.56 (<i>d</i> , 6.8)	18.55	1, 9	1, 3, 8-OCH ₃
3-CH ₃	1.13 (<i>d</i> , 6.4)	19.09	3, 4	3, 4 _{ax} , 4 _{eq} , 2''-OCH₃
8-OCH ₃	3.93 (<i>s</i>)	56.21		7, 1-CH ₃
2'-CH ₃	2.27 (<i>s</i>)	22.21	1', 2', 3', 9'	1', 3', 8'''-OCH₃
4'-OCH ₃	4.09 (<i>s</i>)	56.91	4'	3', 7''', 8'''-OCH₃
2''-CH ₃	2.01 (<i>s</i>)	22.77	1'', 2'', 3''	4 _{eq} , 3'', 1-CH ₃
5''-OCH ₃	4.15 (<i>s</i>)	56.96	5''	6'', 7''
1'''-CH ₃	1.39 (<i>d</i> , 6.8)	18.51	1''', 9'''	1''', 3'''
3'''-CH ₃	1.15 (<i>d</i> , 6.5)	18.98	3''', 4'''	3''', 4''' _{ax} , 4''' _{eq}
8'''-OCH ₃	3.45 (<i>s</i>)	55.63	8'''	1', 3', 1''', 7''', 2'-CH₃, 4'-OCH₃

[a] Multiplicities and coupling constants *J* [Hz] are shown in parentheses, δ values are given in ppm.

[b] ROESY correlations between **2a** and **2b** are marked in bold.

Figures S4a-c. ^1H NMR spectroscopic data of **1** in MeOD.

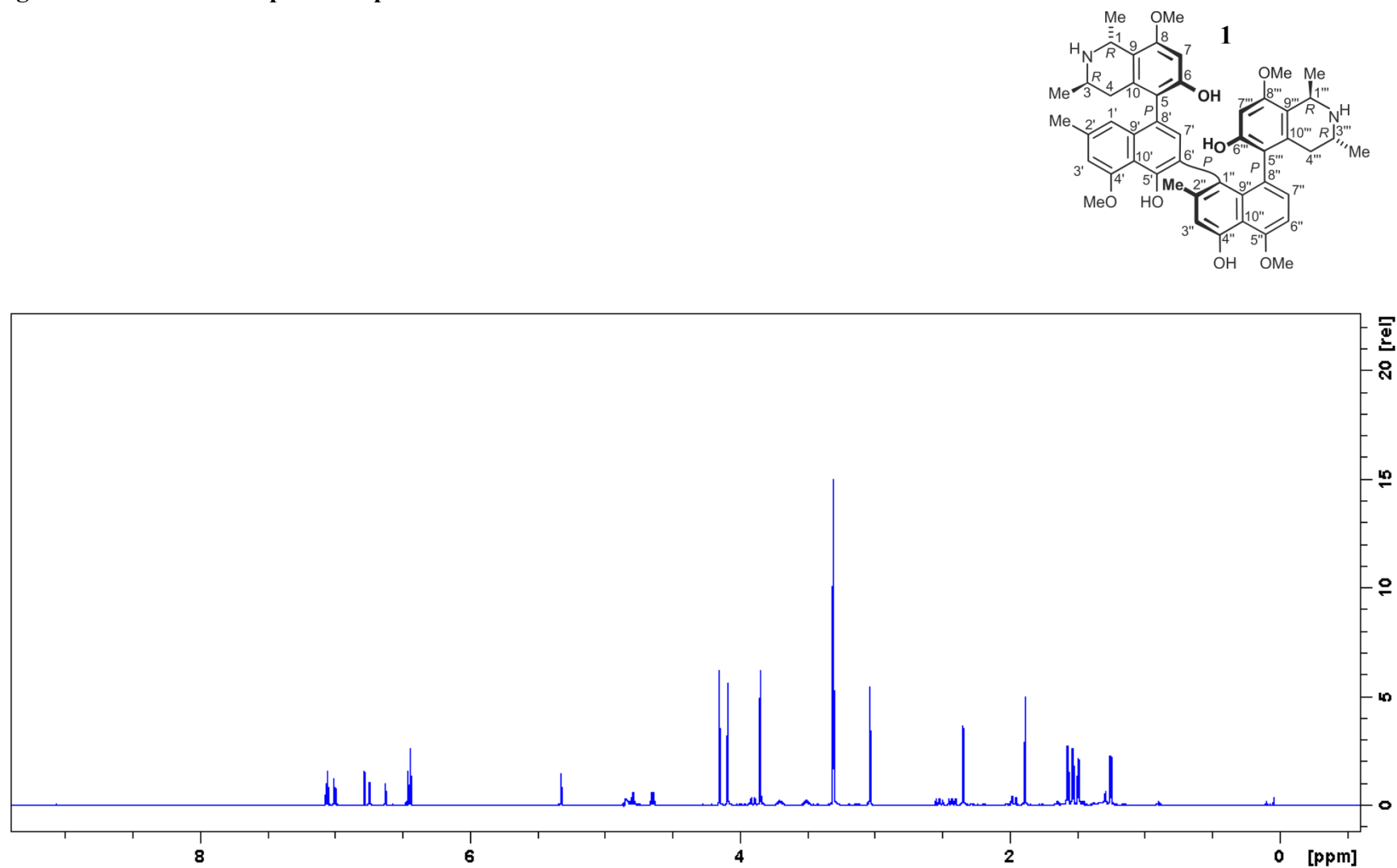


Figure S4a. Overall ^1H NMR spectrum of **1**

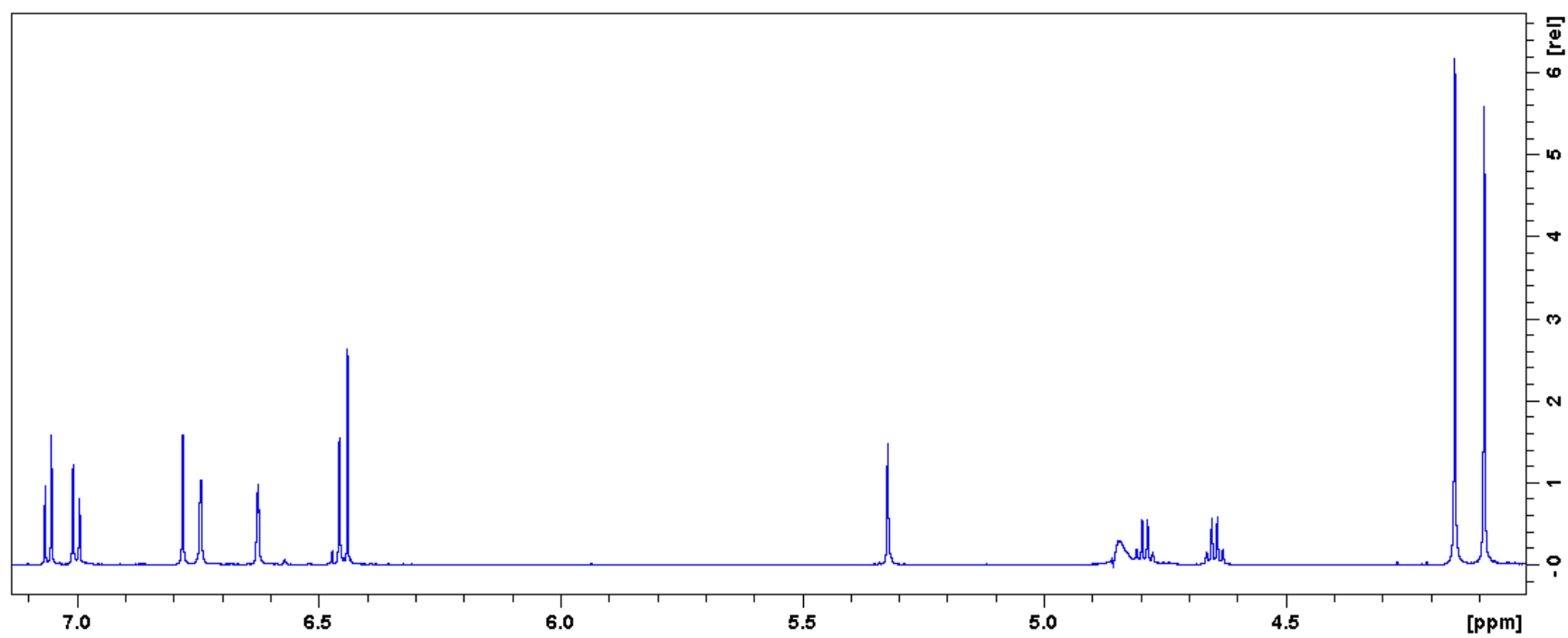


Figure S4b. ^1H NMR spectrum of **1** from 7.1 to 4.0 ppm

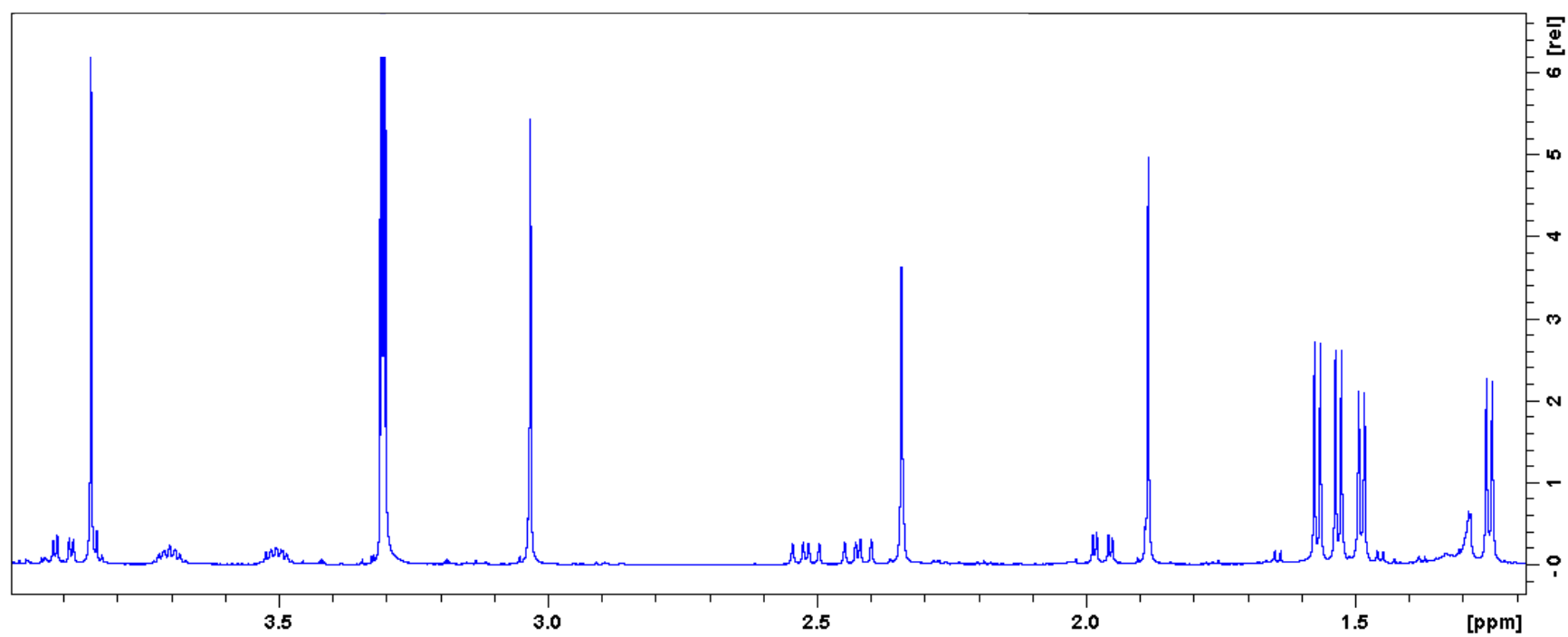


Figure S4c. ^1H NMR spectrum of **1** from 4.0 to 1.2 ppm

Figures S5a-c. ^{13}C NMR spectroscopic data of **1** in MeOD.

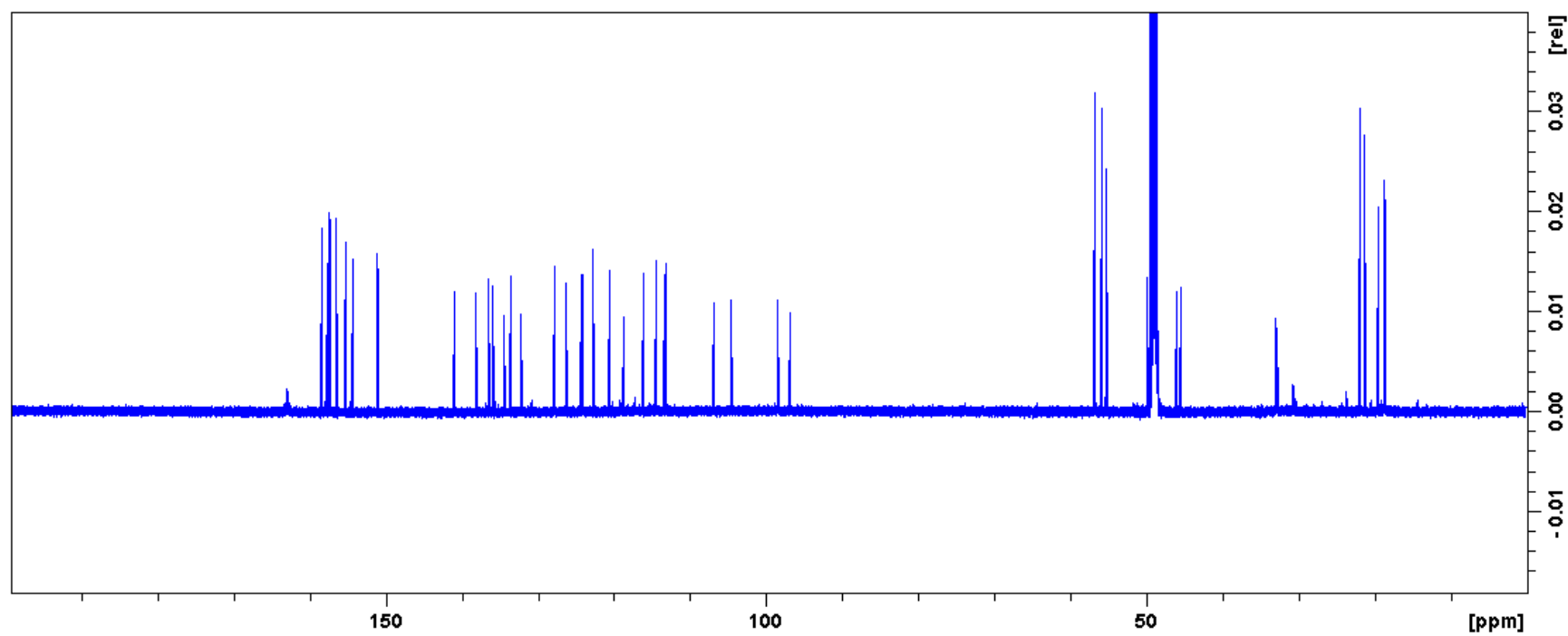
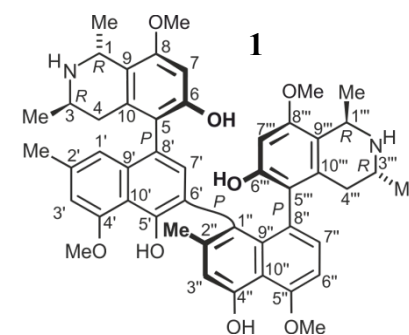


Figure S5a. Overall ^{13}C NMR spectrum of **1**

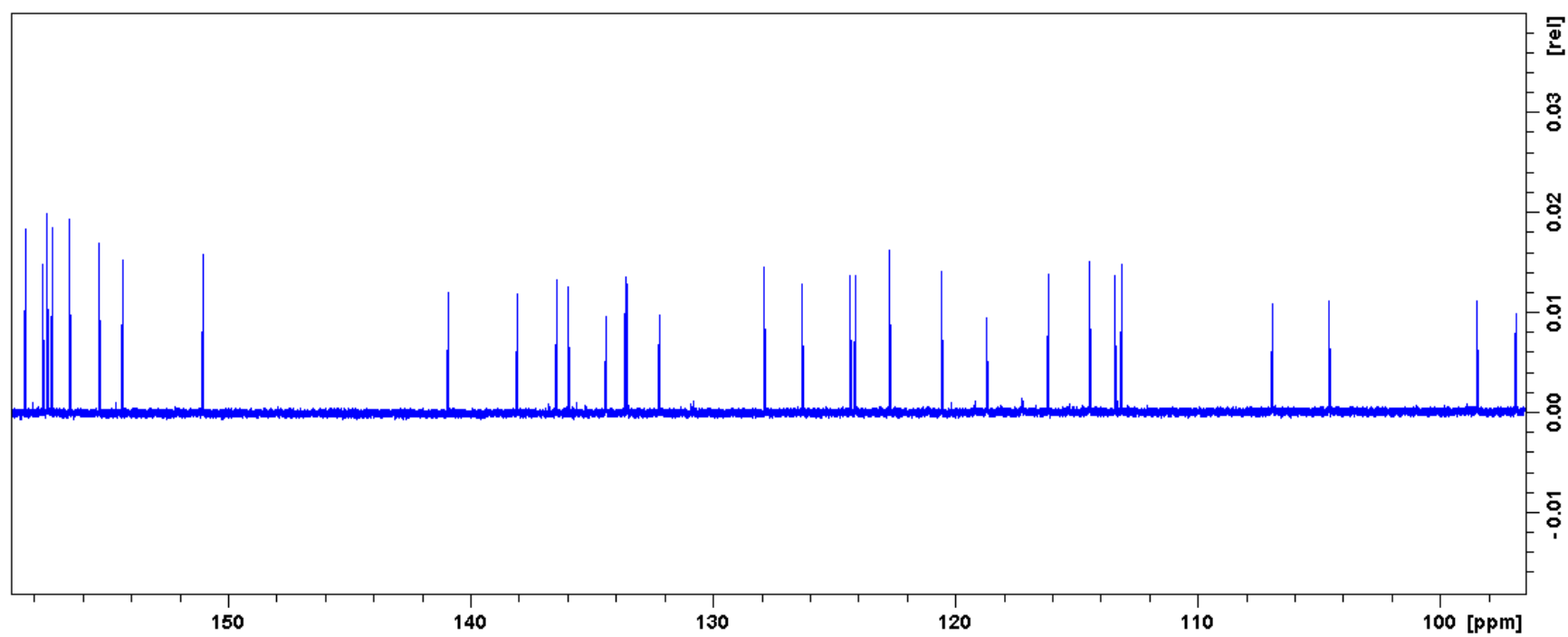


Figure S5b. ^{13}C NMR spectrum of **1** from 95 to 160 ppm

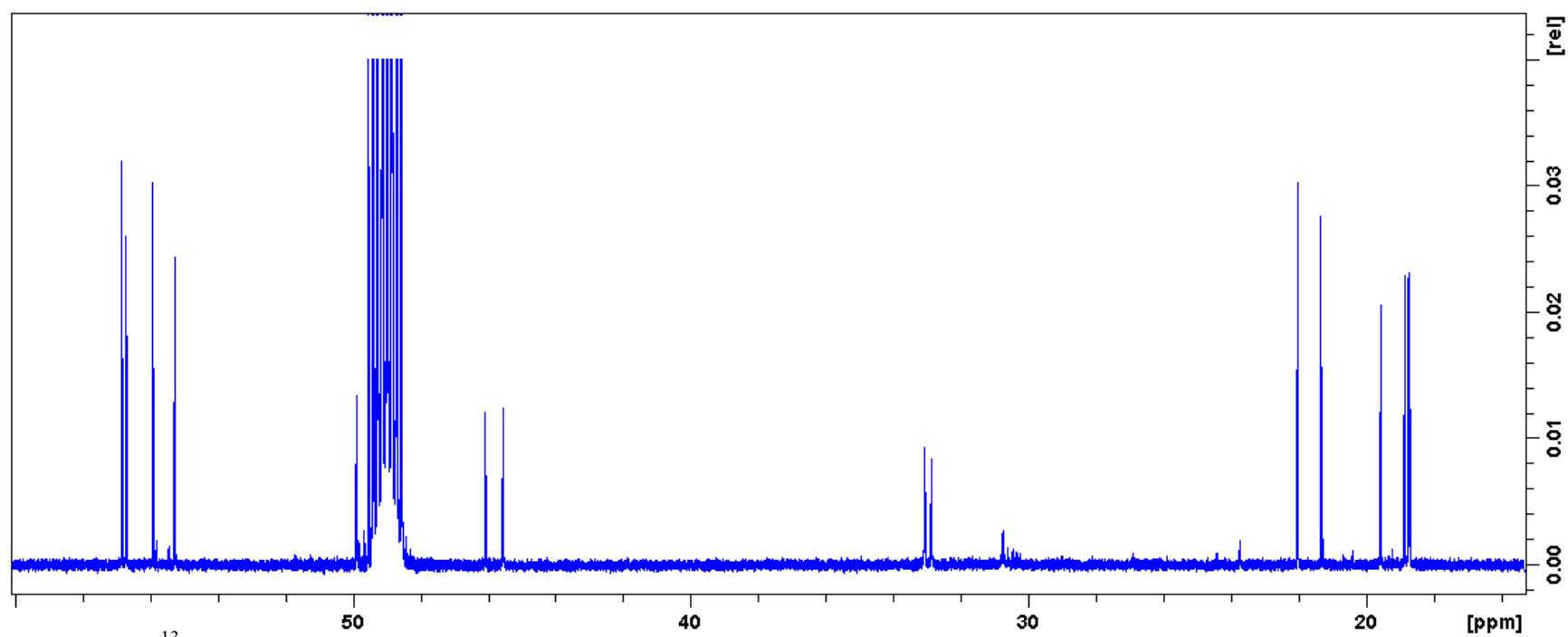


Figure S5c. ^{13}C NMR spectrum of **1** from 60 to 16 ppm

Figures S6a-c. DEPT 135 NMR spectroscopic data of **1** in MeOD.

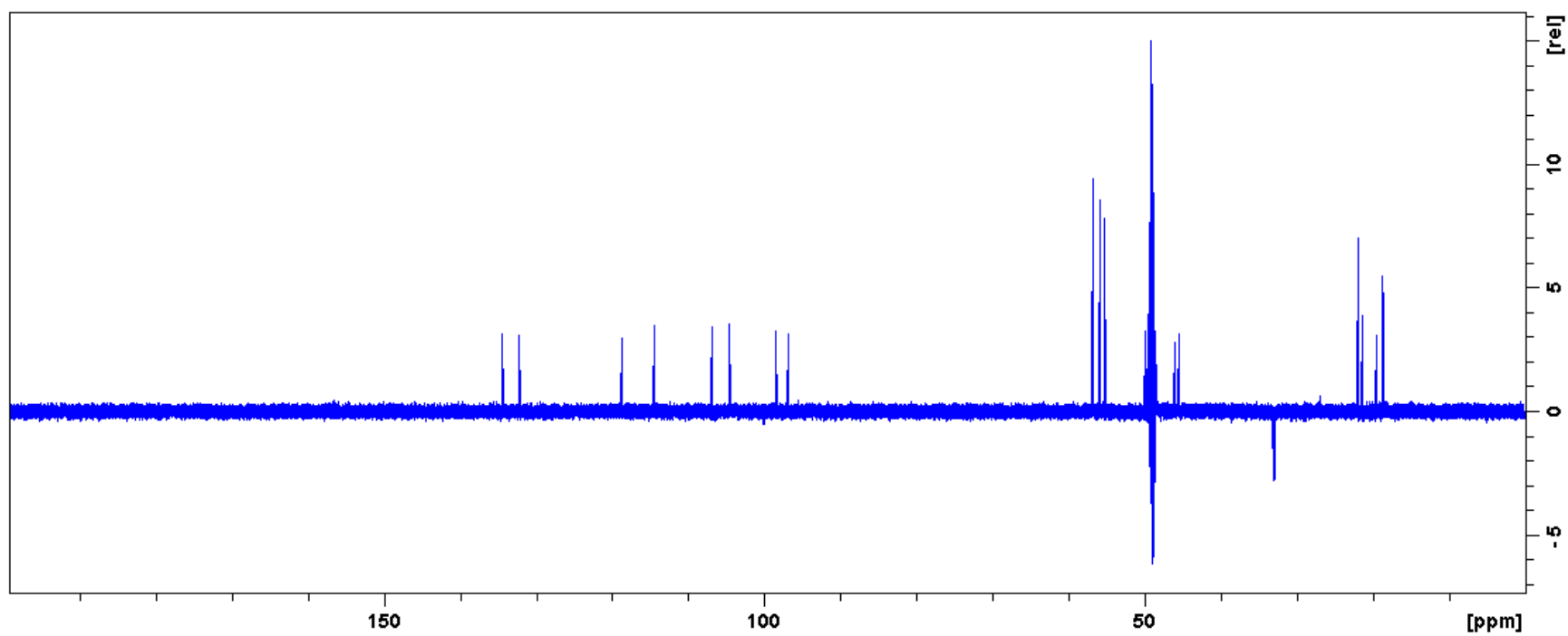
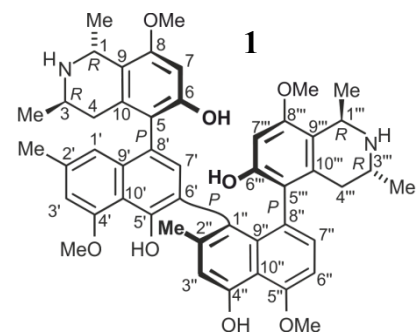


Figure S6a. Overall DEPT 135 NMR spectrum of **1**

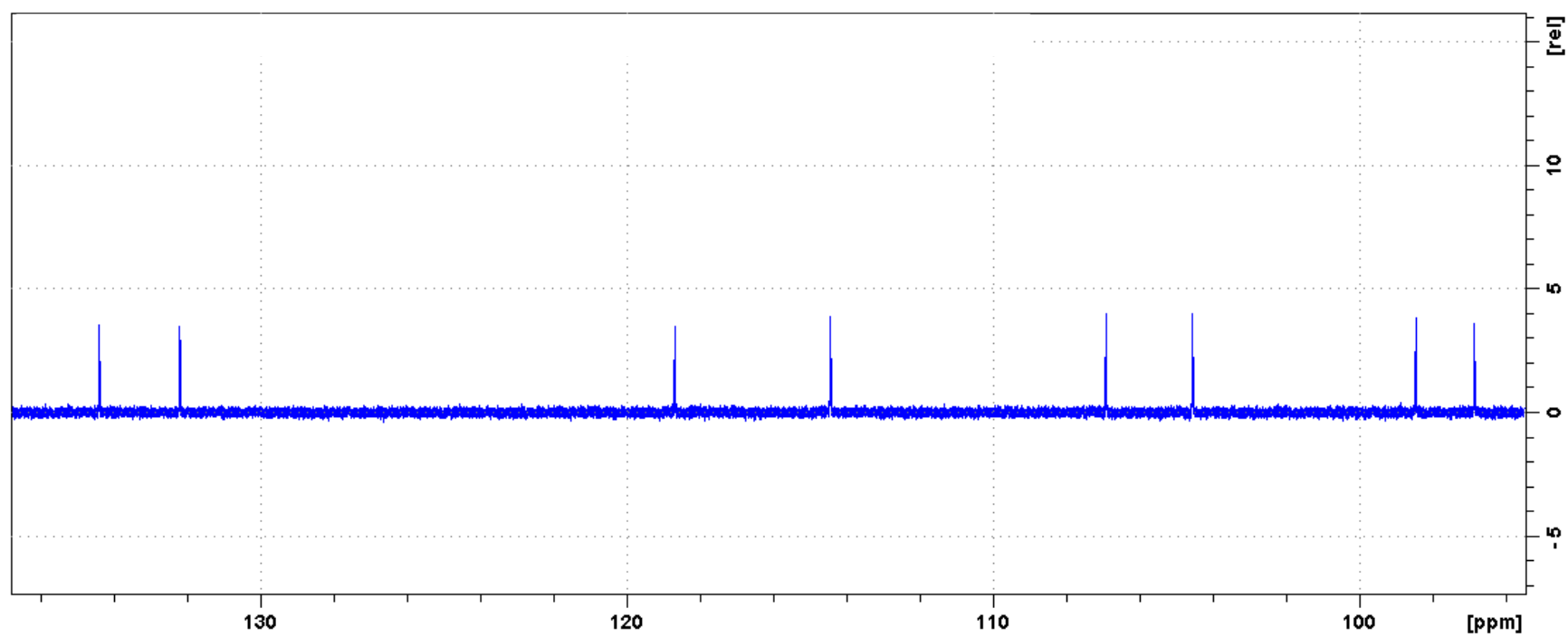


Figure S6b. DEPT 135 NMR spectrum of **1** from 95 to 140

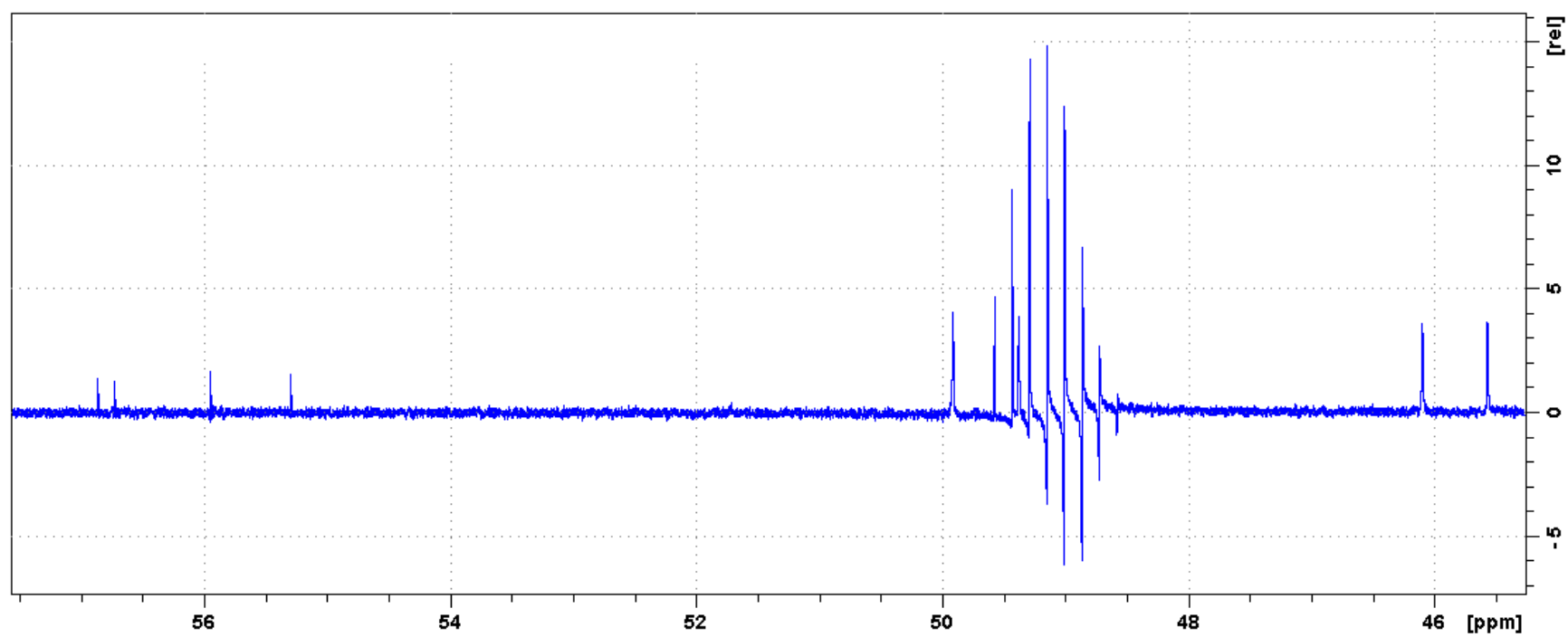


Figure S6c. DEPT 135 NMR spectrum of **1** from 48 to 60 ppm

Figures S7a-c. COSY spectra of **1** in MeOD.

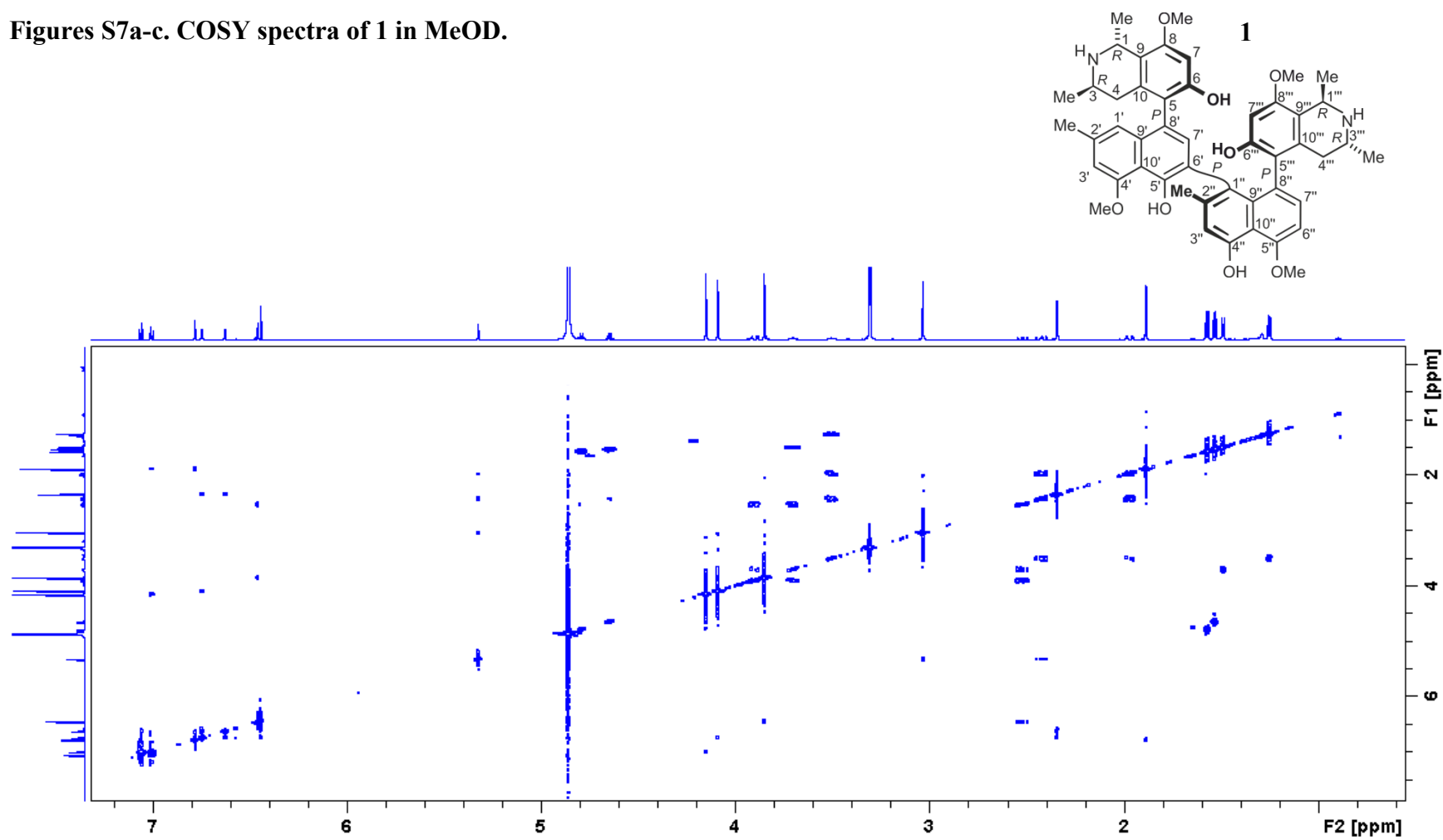


Figure S7a. Overall COSY spectrum of **1**

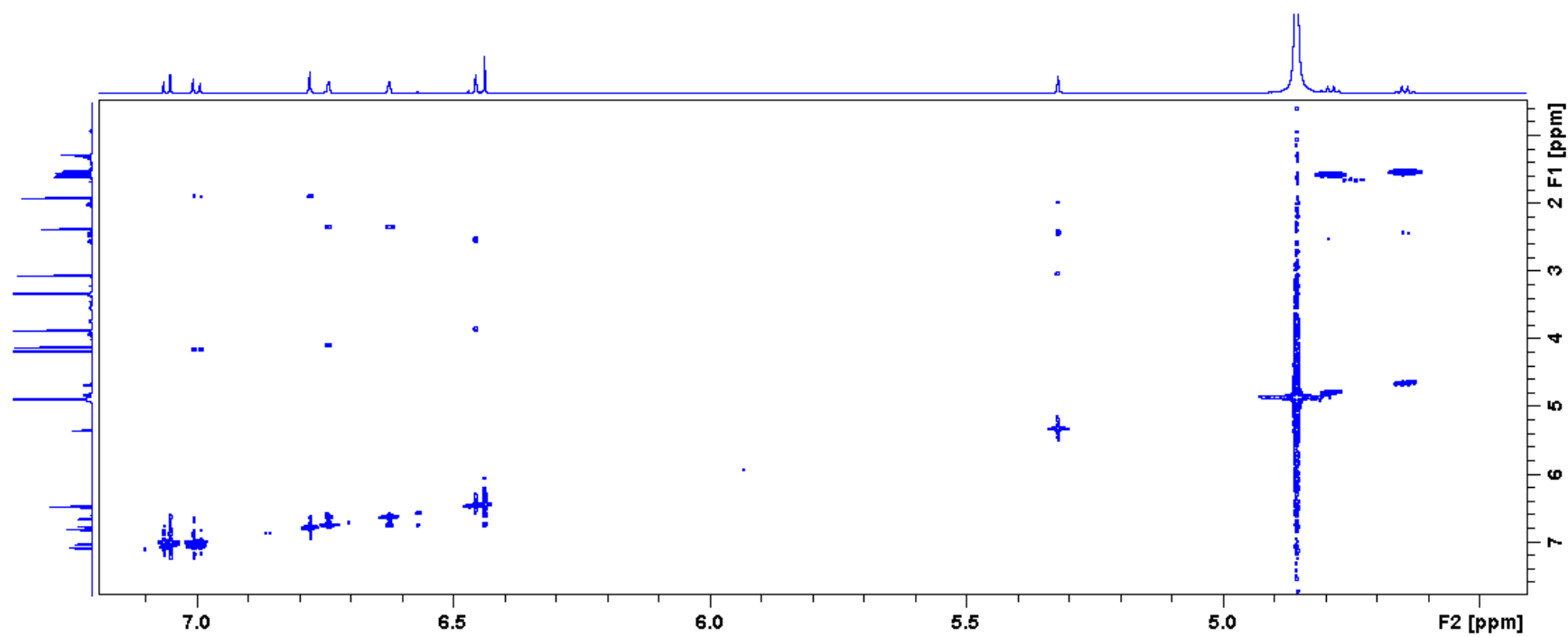


Figure S7b. COSY spectrum of **1** from 7.1 to 4.2 ppm

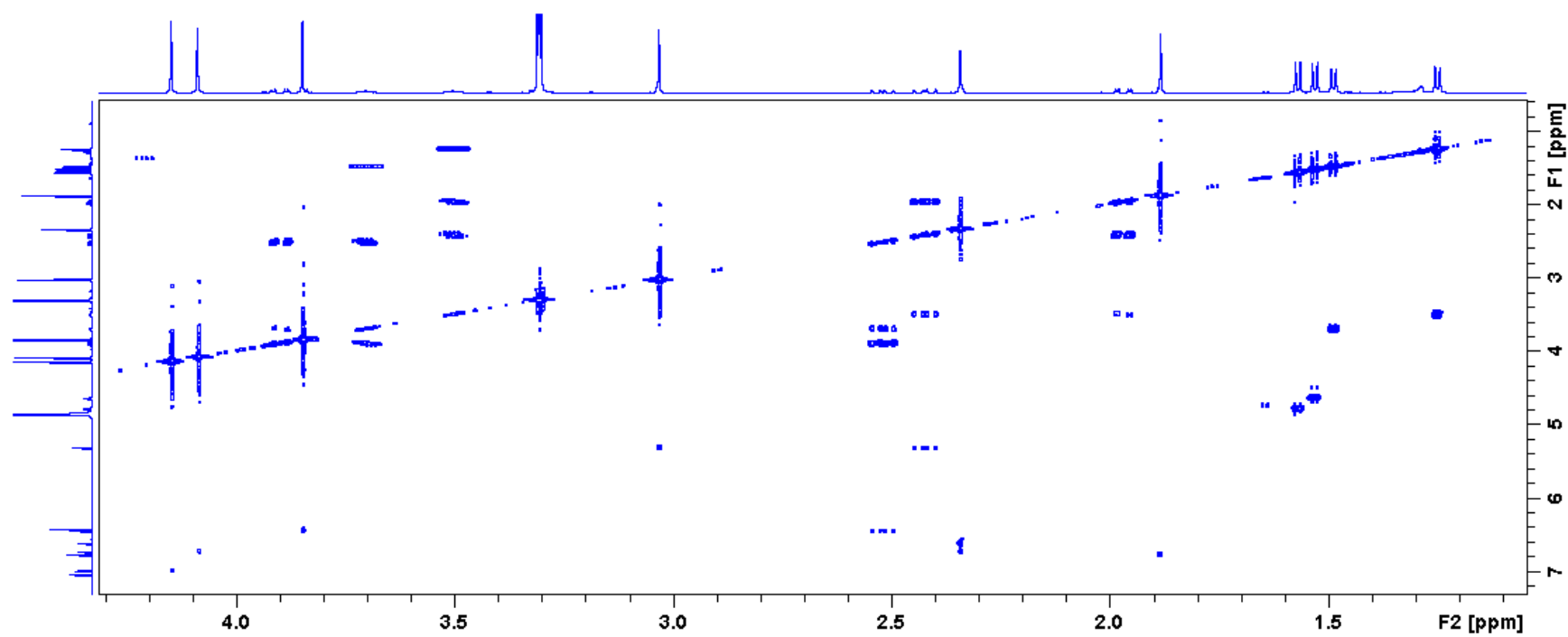


Figure S7c. COSY spectrum of **1** from 4.2 to 1.2 ppm

Figures S8a-c. ROESY spectra of 1 in MeOD.

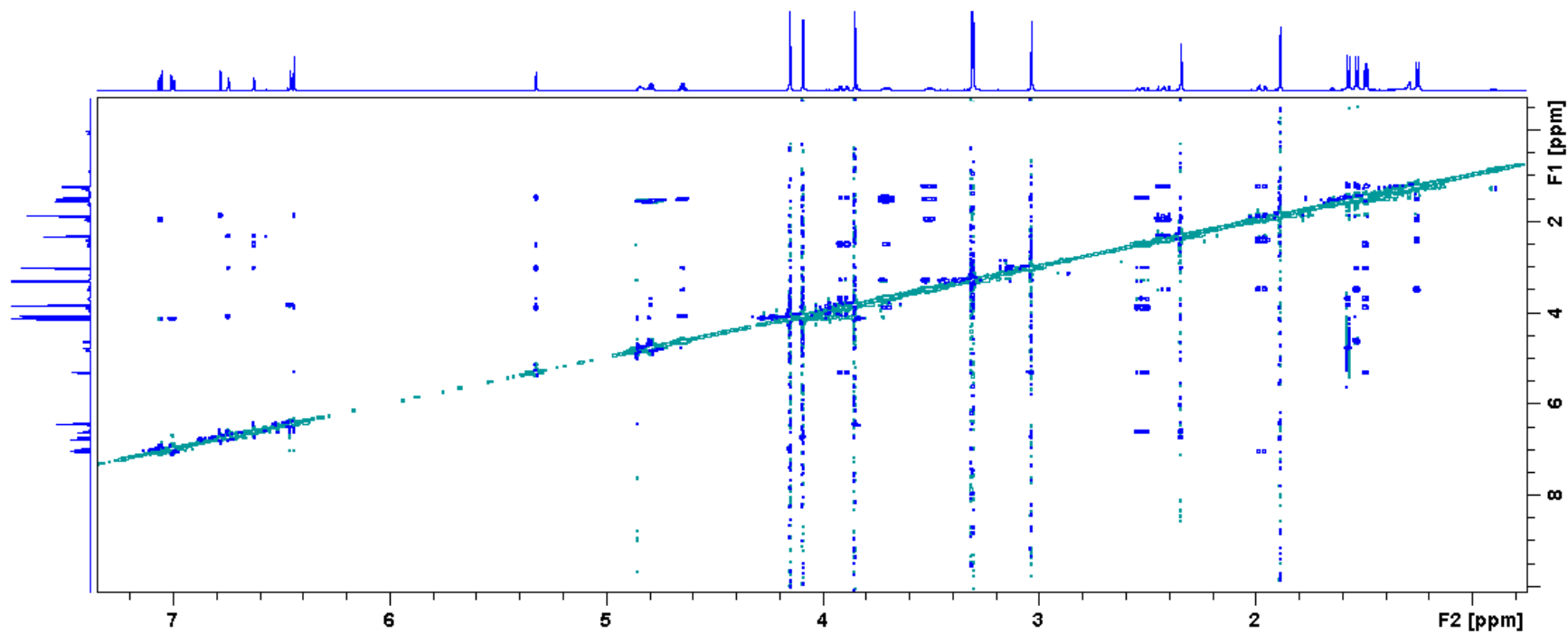
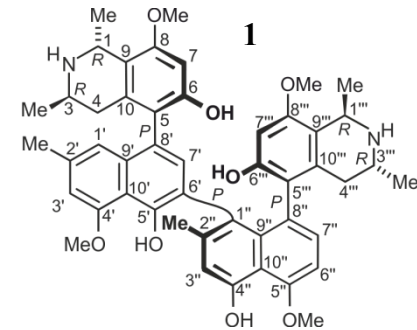


Figure S8a. Overall ROESY spectrum of **1**

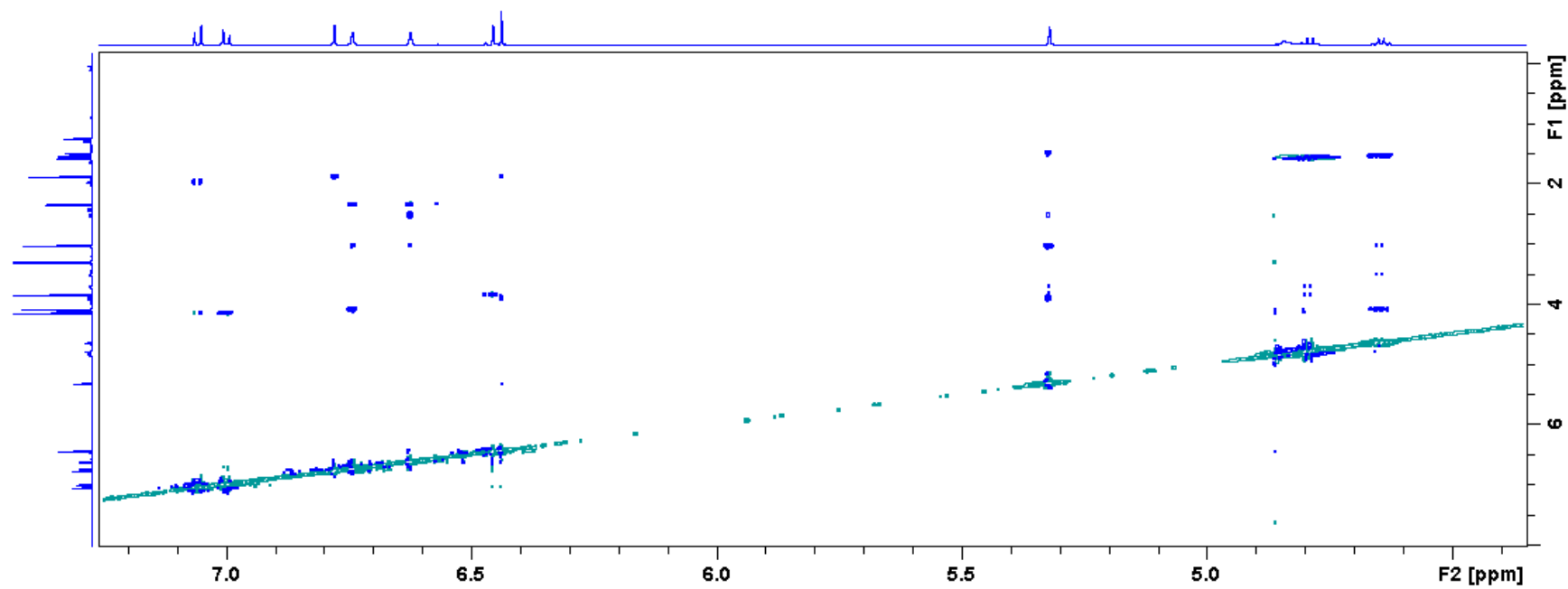


Figure S8b. ROESY spectrum of **1** from 7.2 to 4.2 ppm

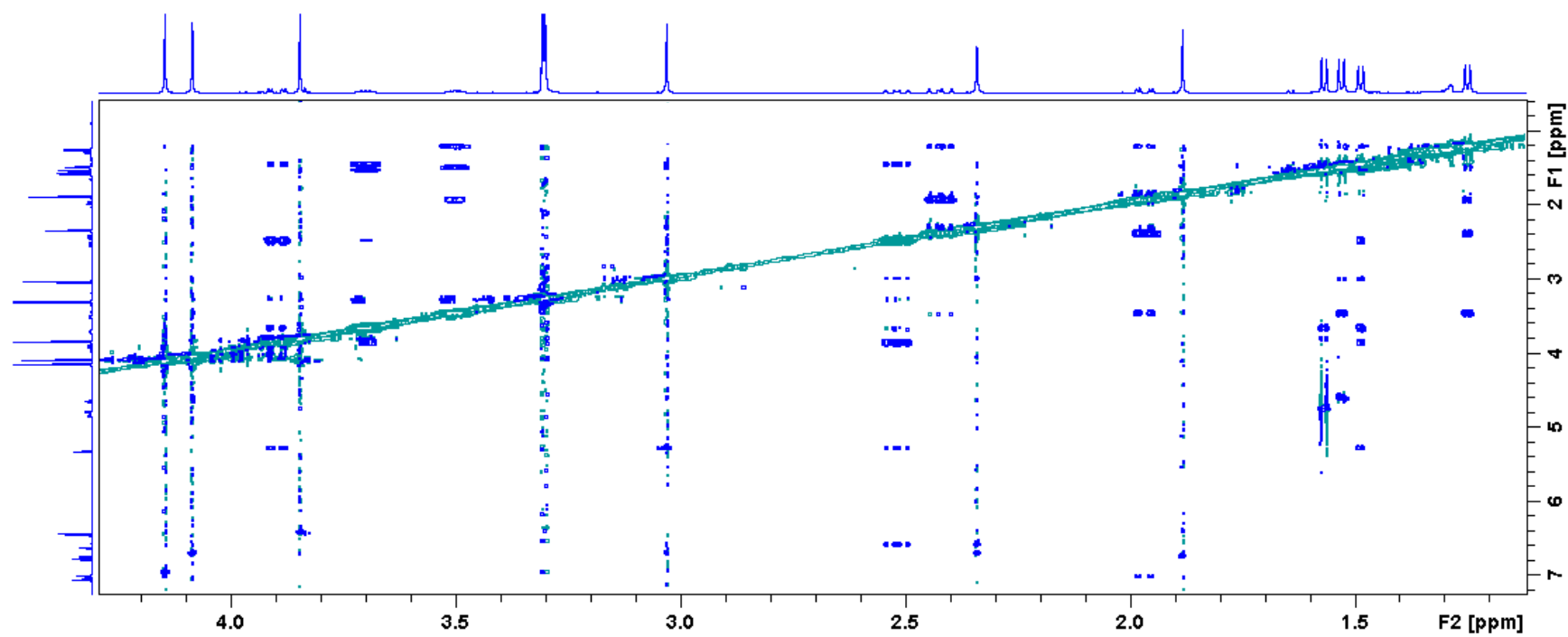


Figure S8c. ROESY spectrum of **1** from 4.2 to 1.2 ppm

Figures S9a-c. HSQC spectra of **1** in MeOD.

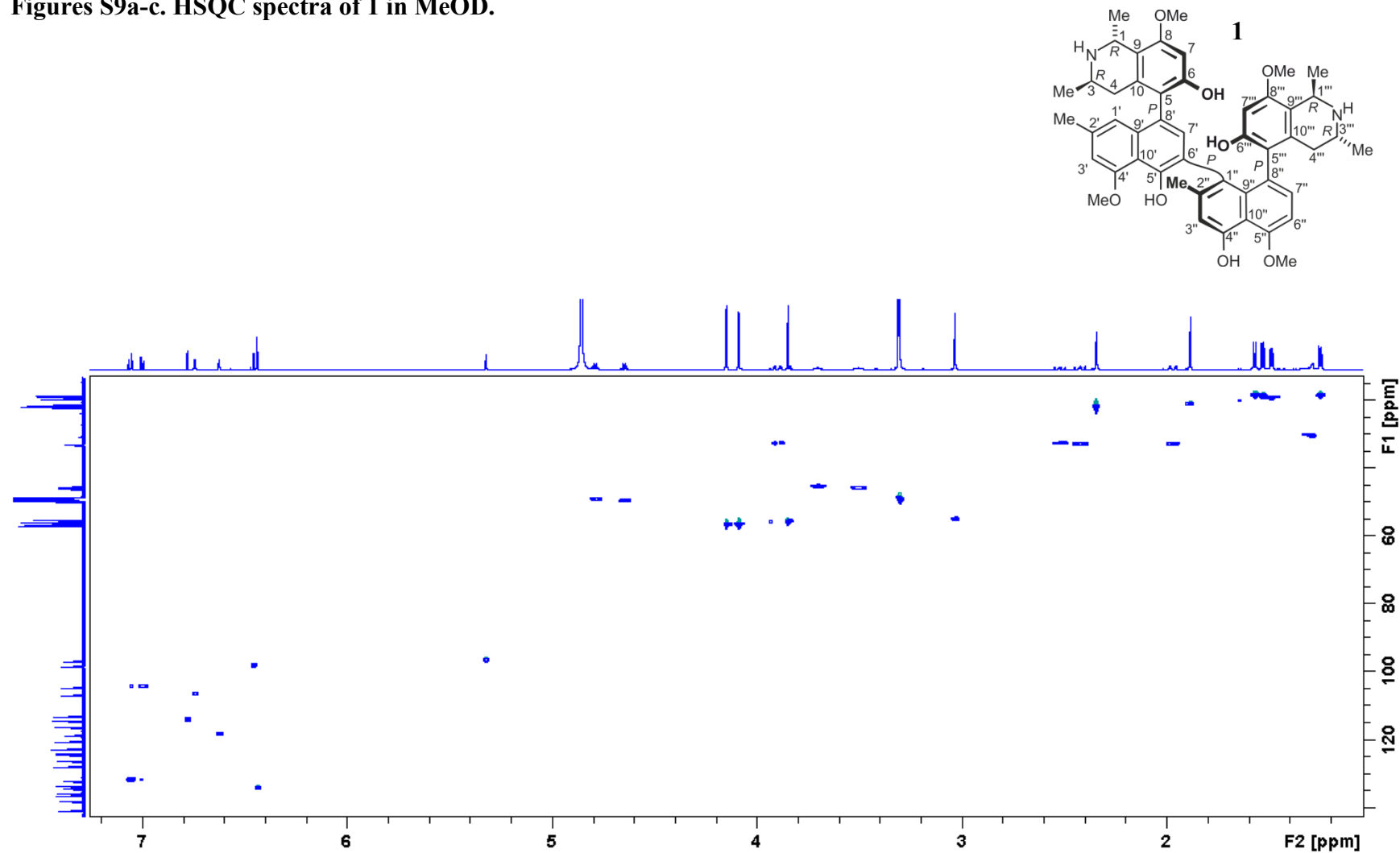


Figure S9a. Overall HSQC spectrum of **1**

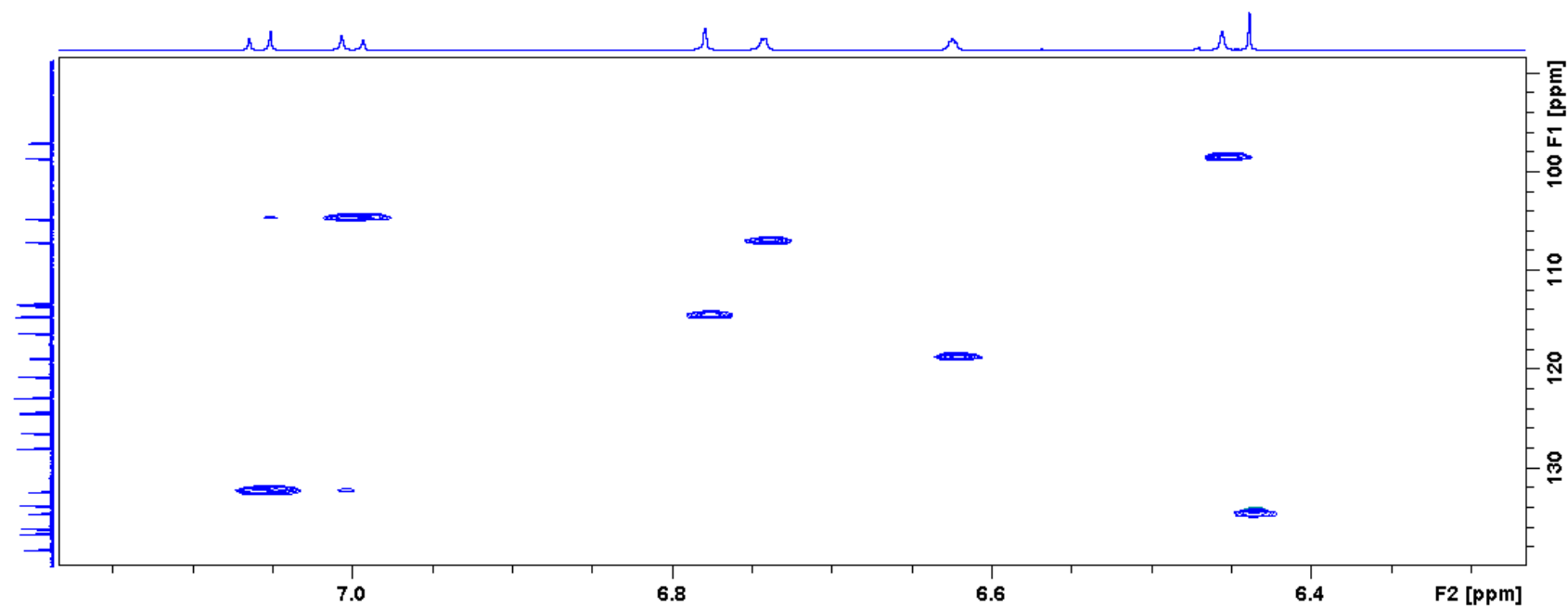


Figure S9b. HSQC spectrum of **1** from 7.3 to 6.0 ppm

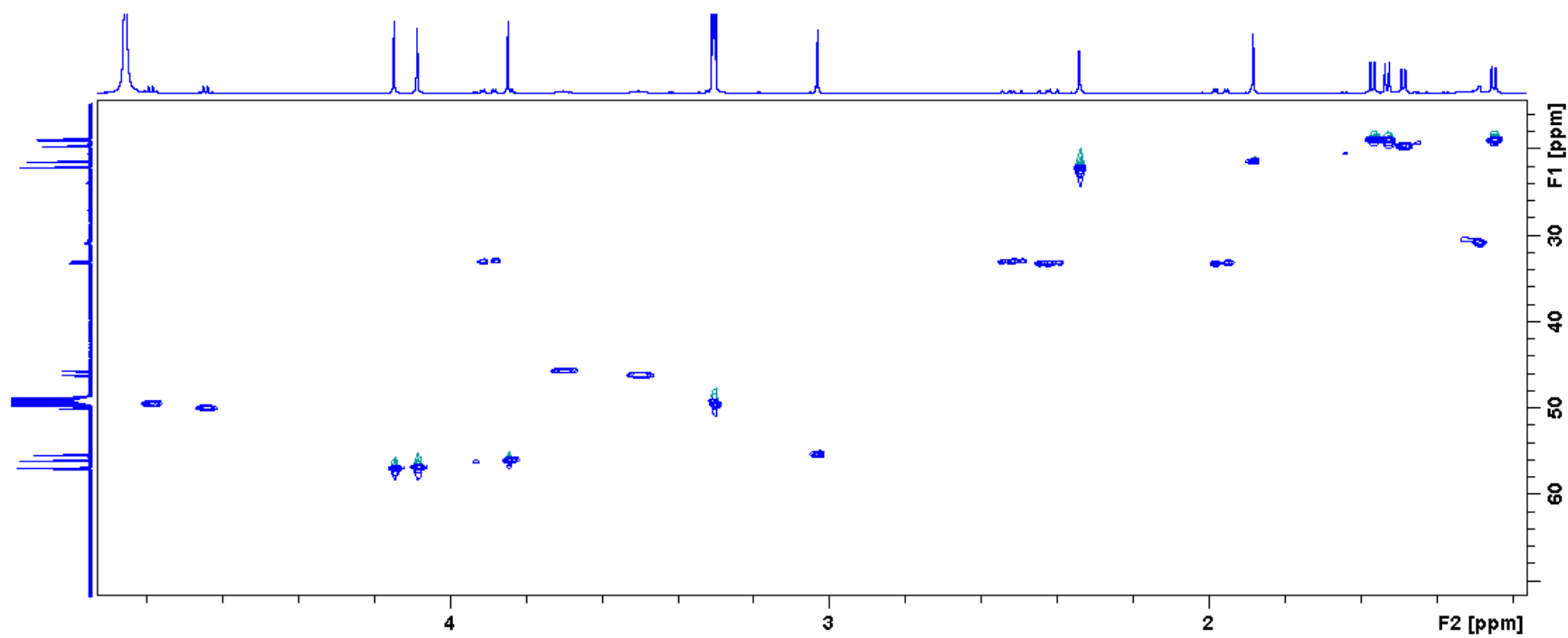


Figure S9c. HSQC spectrum of **1** from 5.0 to 1.2 ppm

Figures S10a-c. HMBC spectra of **1** in MeOD.

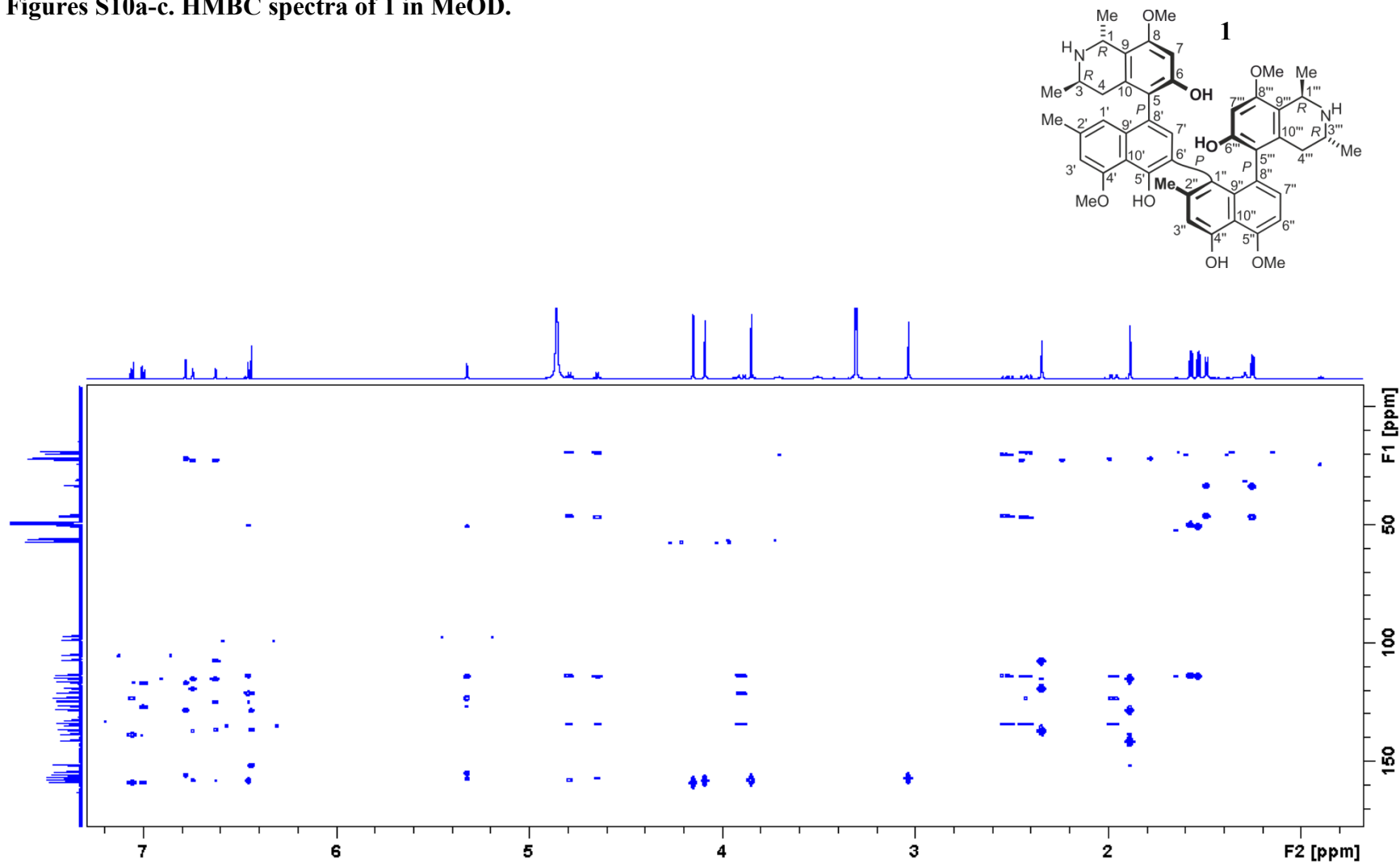


Figure S10a. Overall HMBC spectrum of **1**

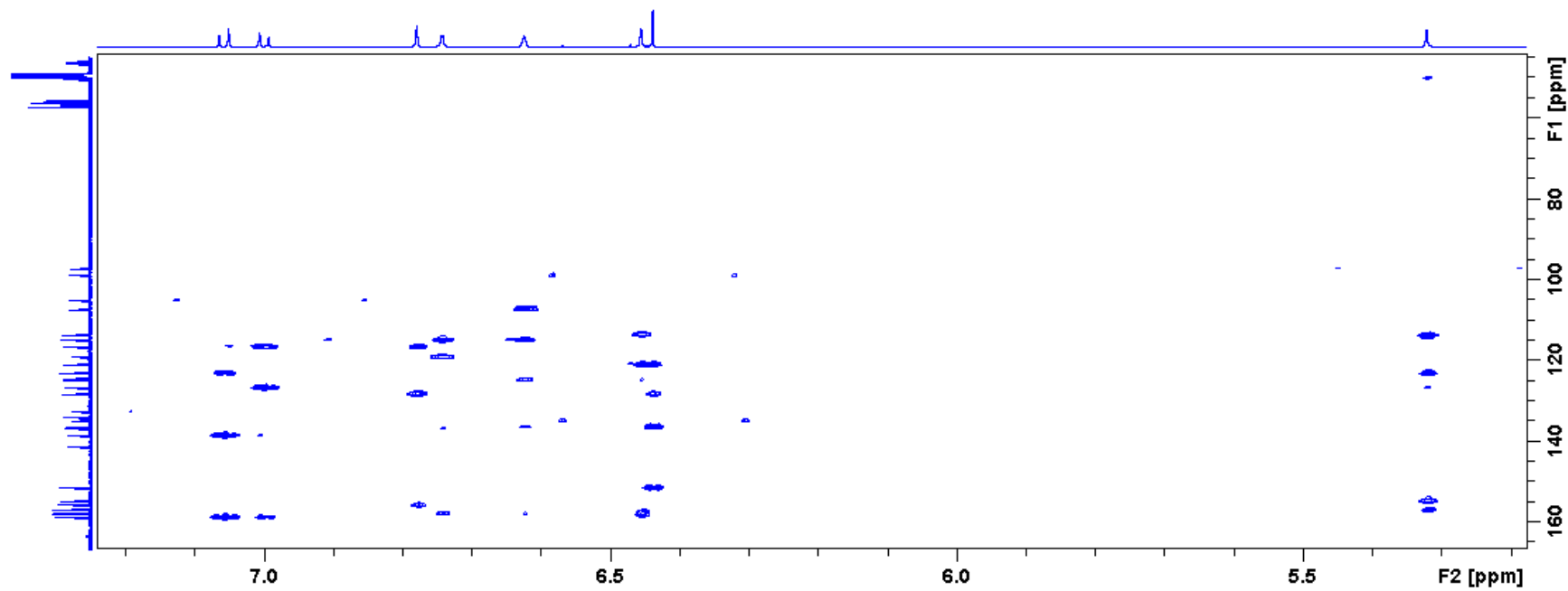


Figure S10b. HMBC spectrum of **1** from 7.2 to 4.6 ppm

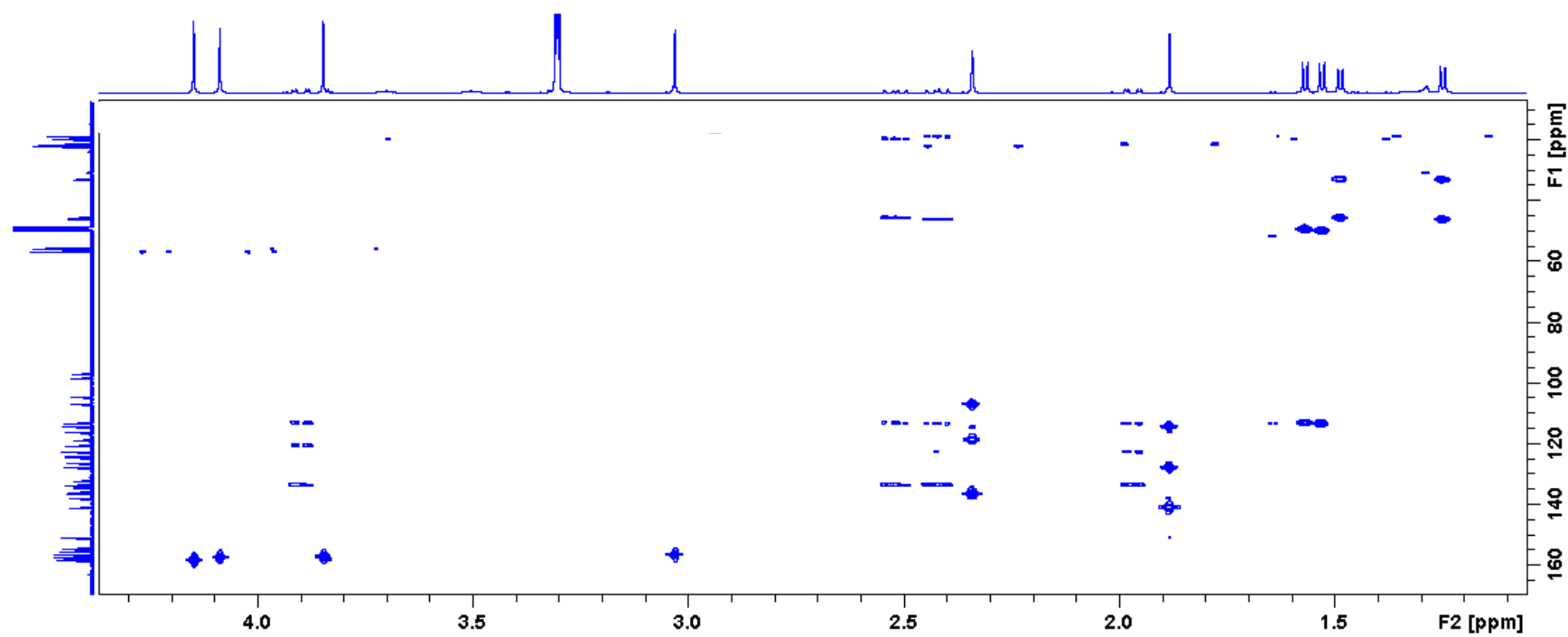
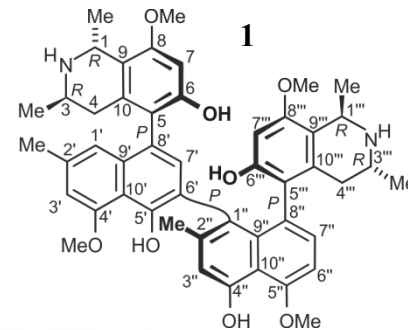


Figure S10c. HMBC spectrum of **1** from 4.6 to 1.1 ppm

Figure S11. HRESIMS spectrum of 1.



Acquisition Parameter

Source Type ESI
Scan Range n/a
Scan Begin 50 m/z
Scan End 2250 m/z

Ion Polarity Positive
Capillary Exit 190.0 V
Hexapole RF 280.0 V
Skimmer 1 50.0 V
Hexapole 1 23.0 V

Set Corrector Fill 49 V
Set Pulsar Pull 802 V
Set Pulsar Push 804 V
Set Reflector 1700 V
Set Flight Tube 8600 V
Set Detector TOF 2020 V

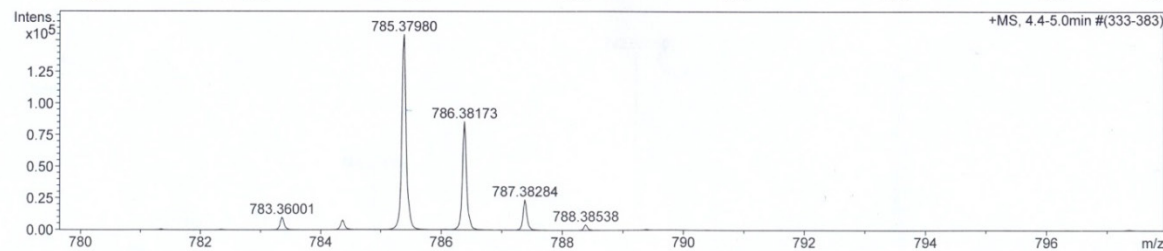
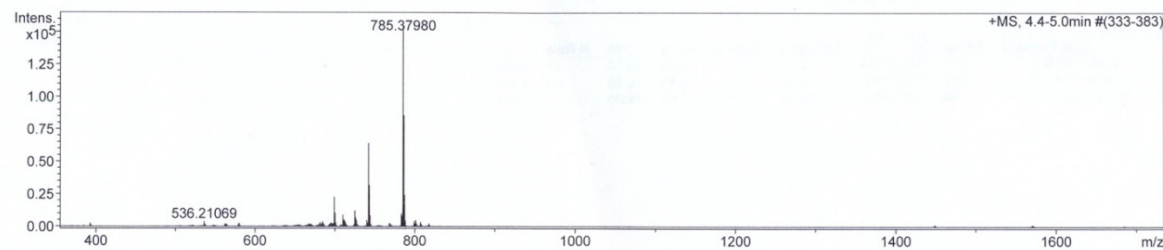


Figure S12. IR spectrum of 1.

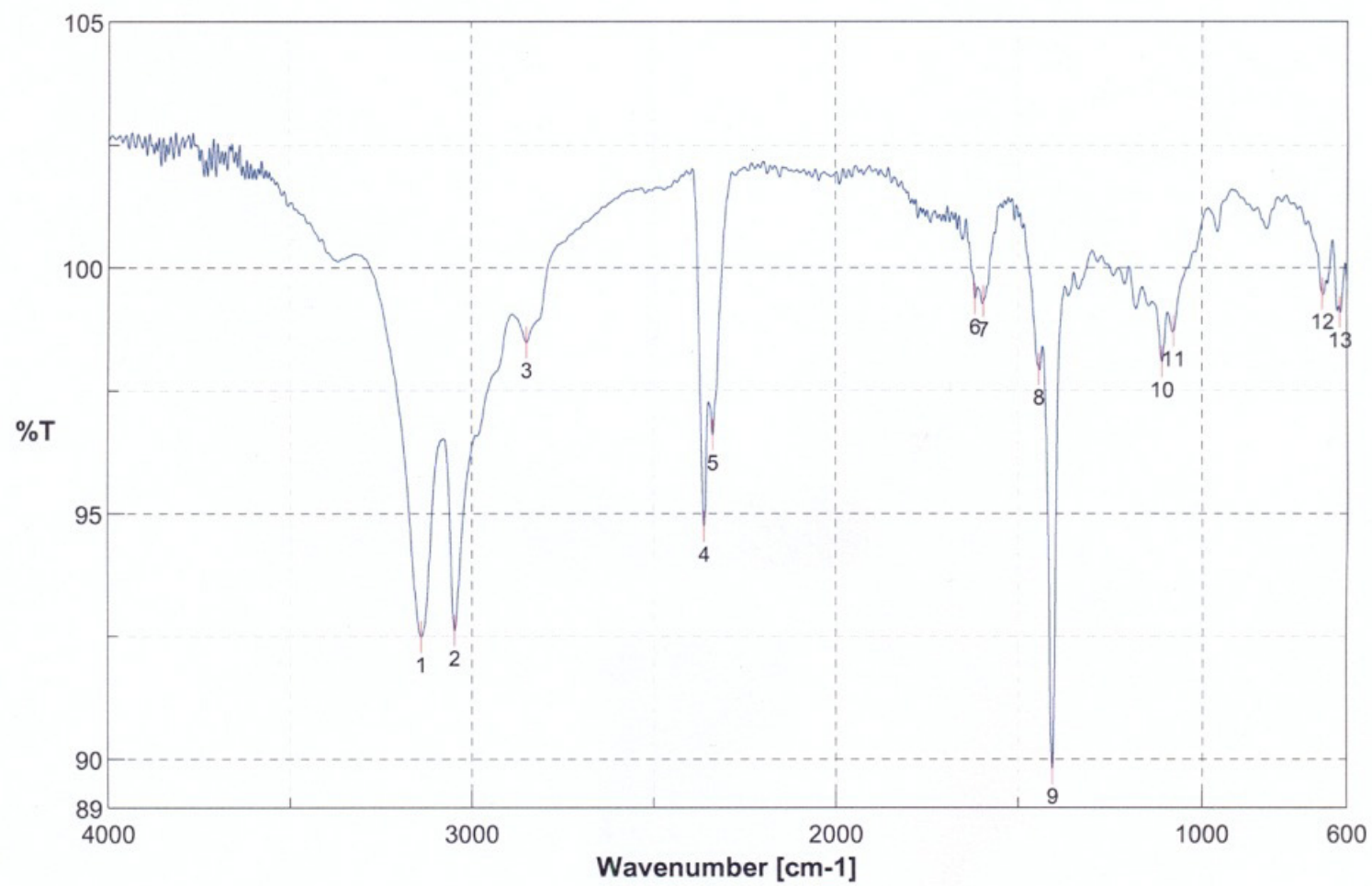


Figure S13. CD spectrum of 1.

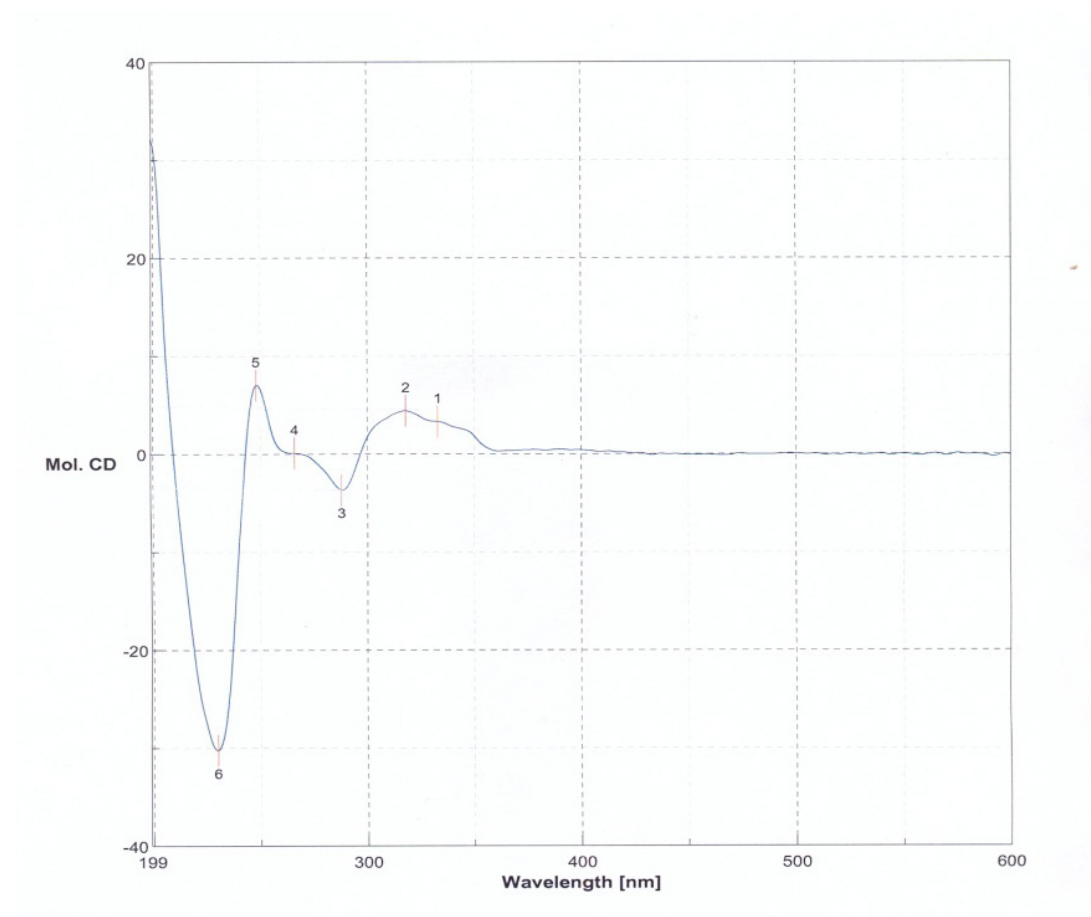
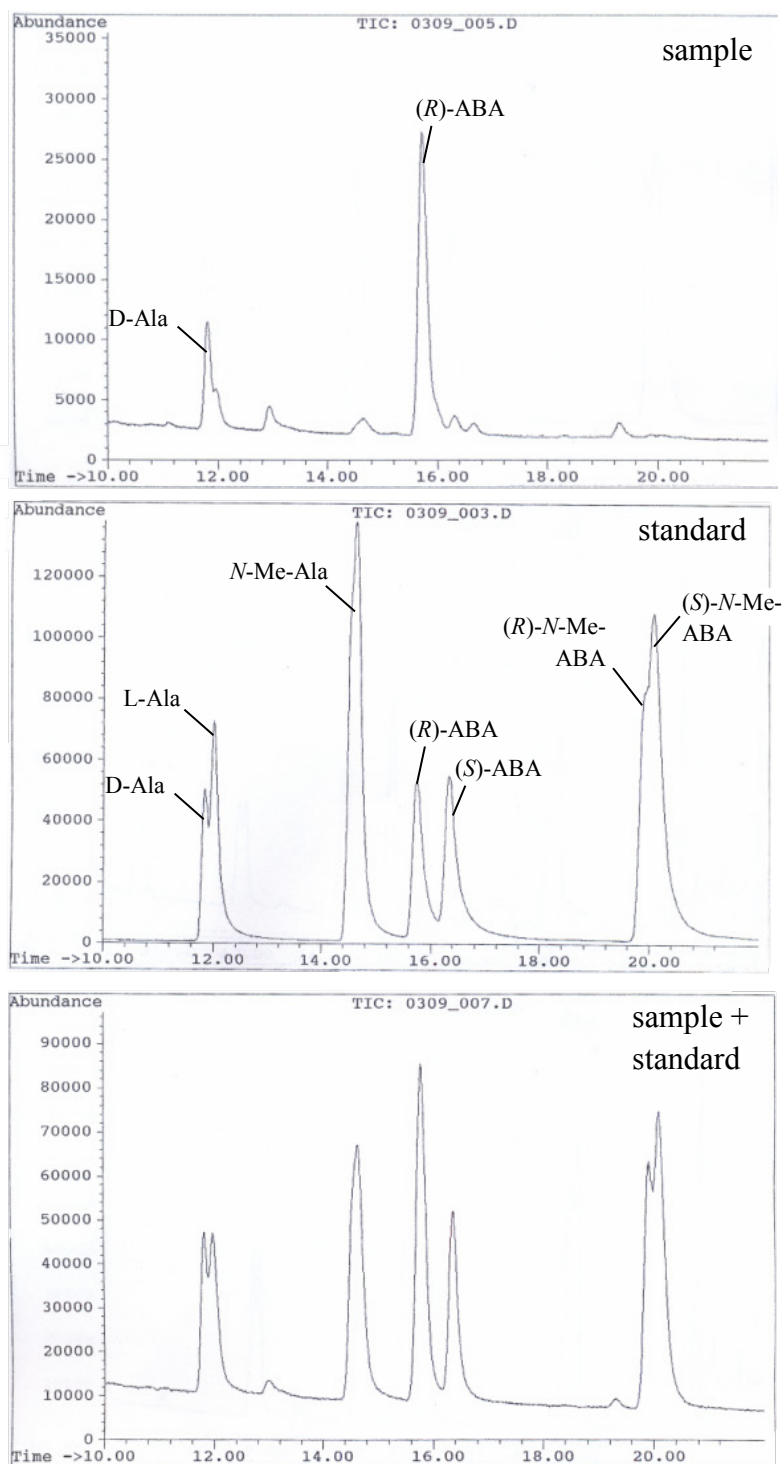


Figure S14. Oxidative degradation products of 1.



Ala = Alanine

N-Me-Ala = *N*-Methylalanine

ABA = 3-Aminobutyric acid

N-Me-ABA = *N*-Methyl-3-aminobutyric acid

Figures S15a-c. ^1H NMR spectroscopic data of **2** in MeOD.

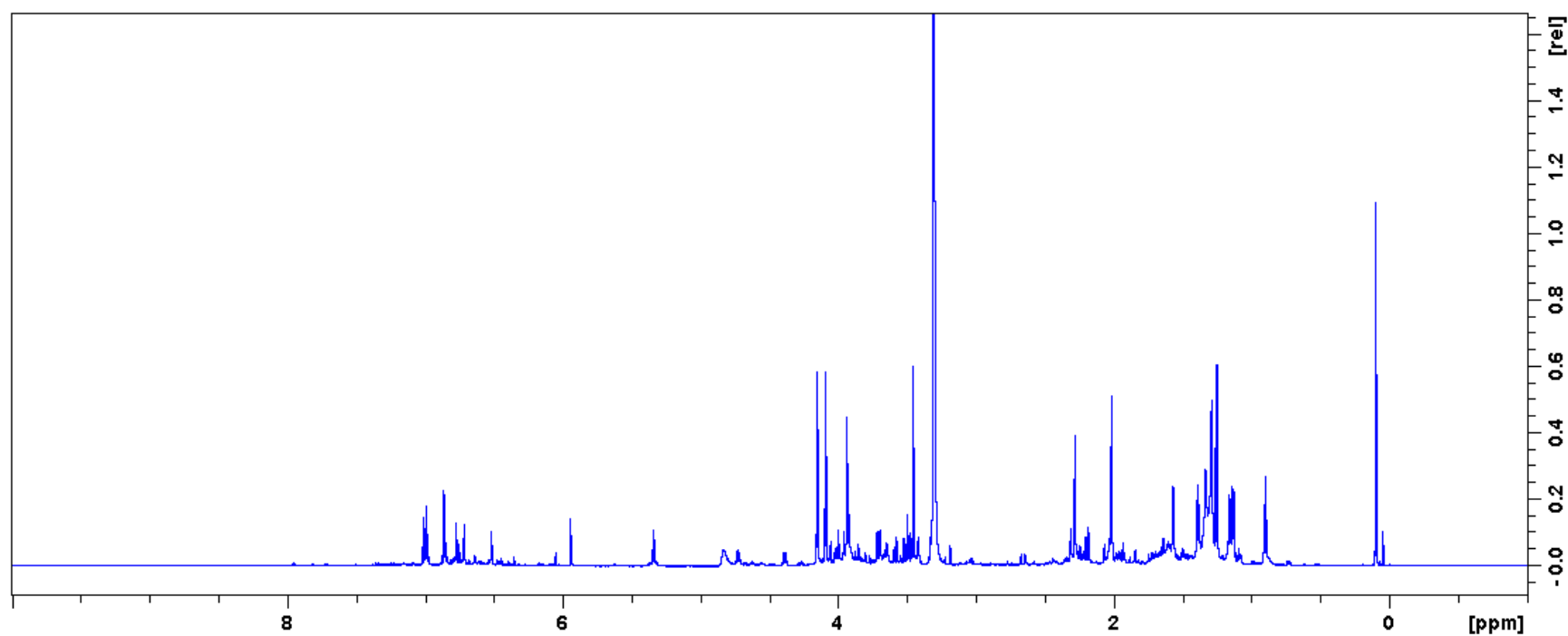
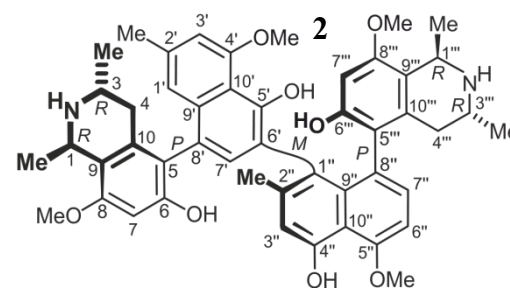


Figure S15a. Overall ^1H spectrum of **2**

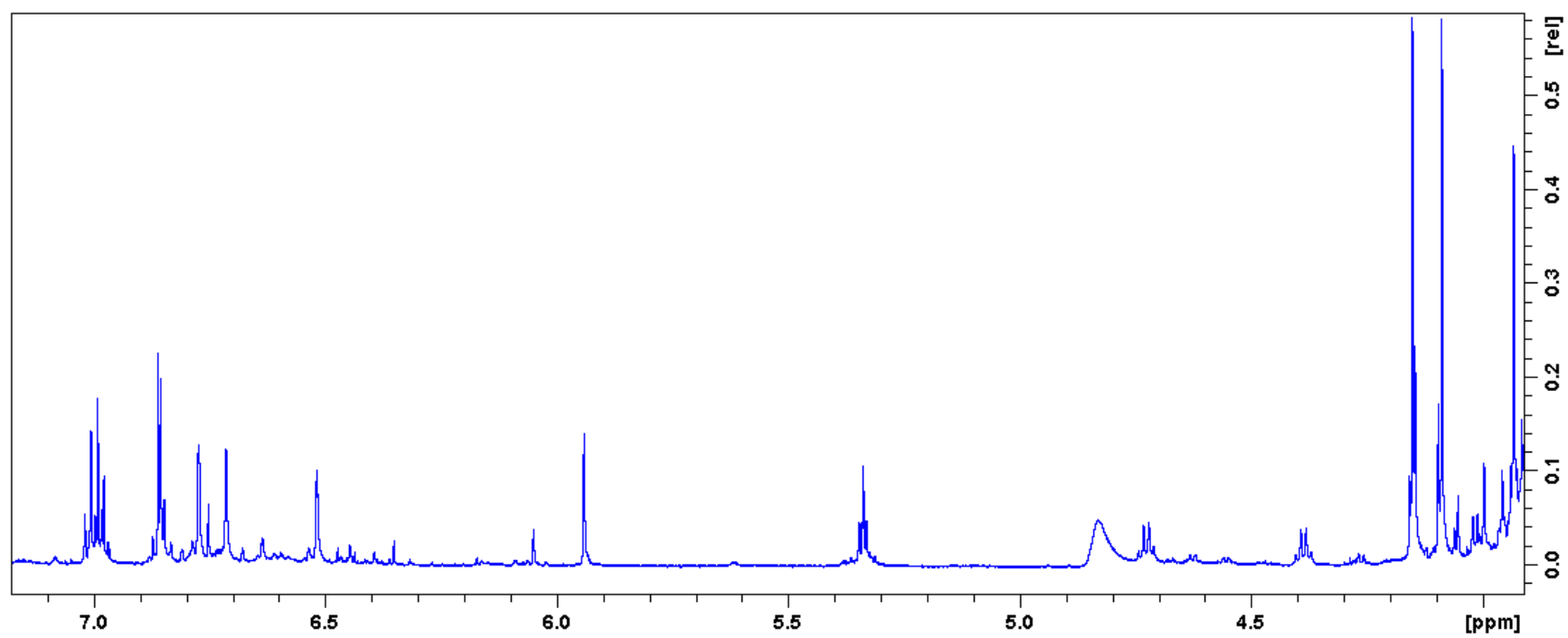


Figure S15b. ^1H spectrum of **2** from 7.1 to 4.0 ppm

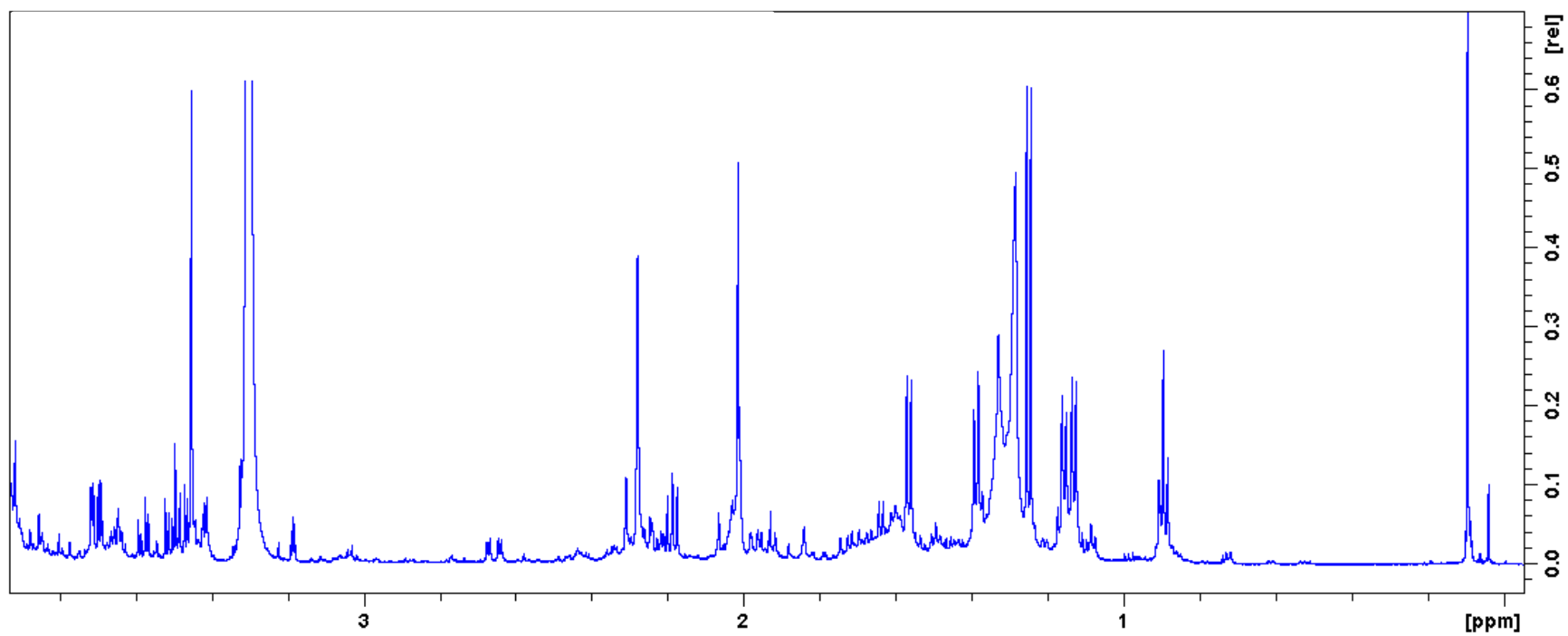


Figure S15c. ^1H spectrum of **2** from 4.0 to 0.0 ppm

Figures S16a-c. ^{13}C NMR spectroscopic data of **2** in MeOD.

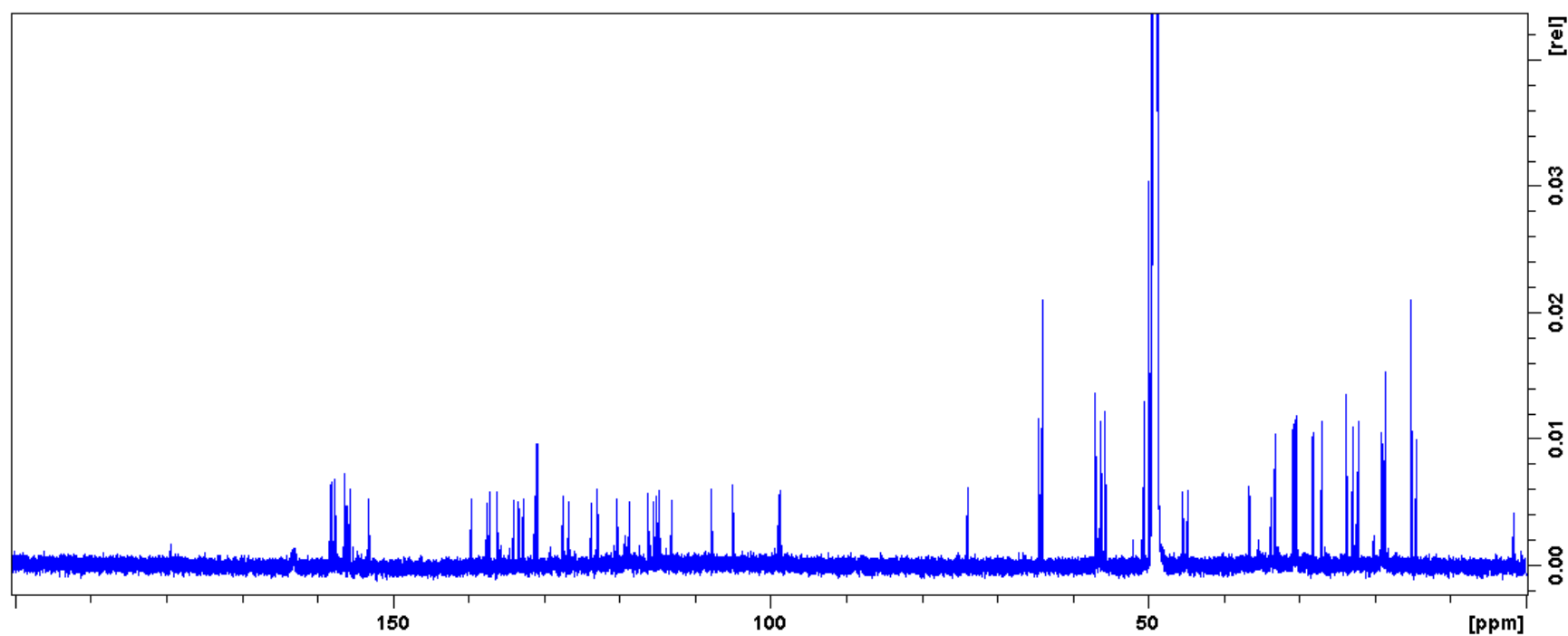
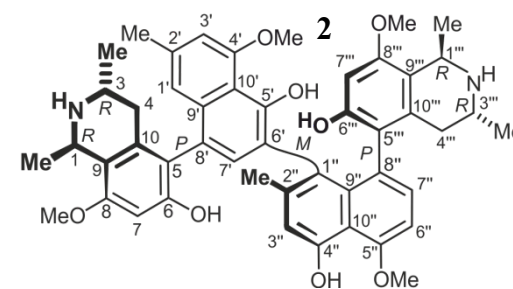


Figure S16a. Overall ^{13}C spectrum of **2**

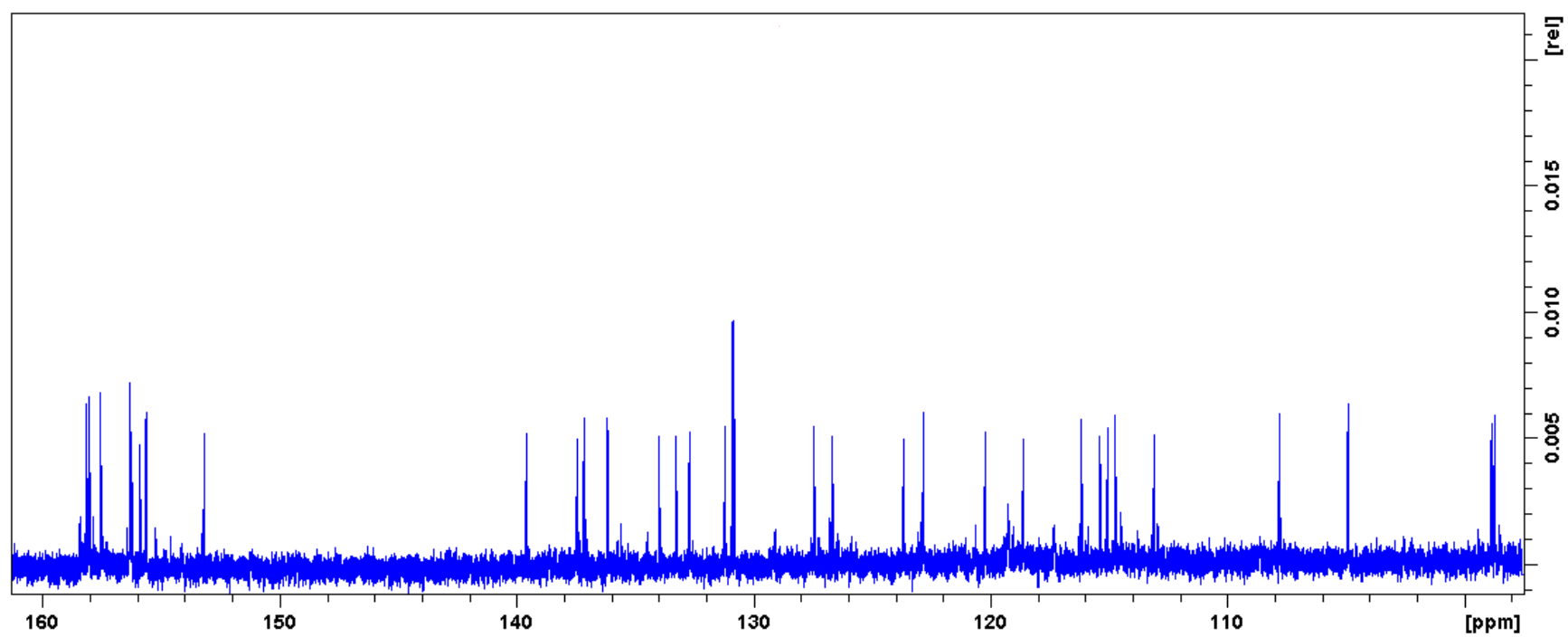


Figure S16b. ^{13}C spectrum of **2** from 160 to 95 ppm

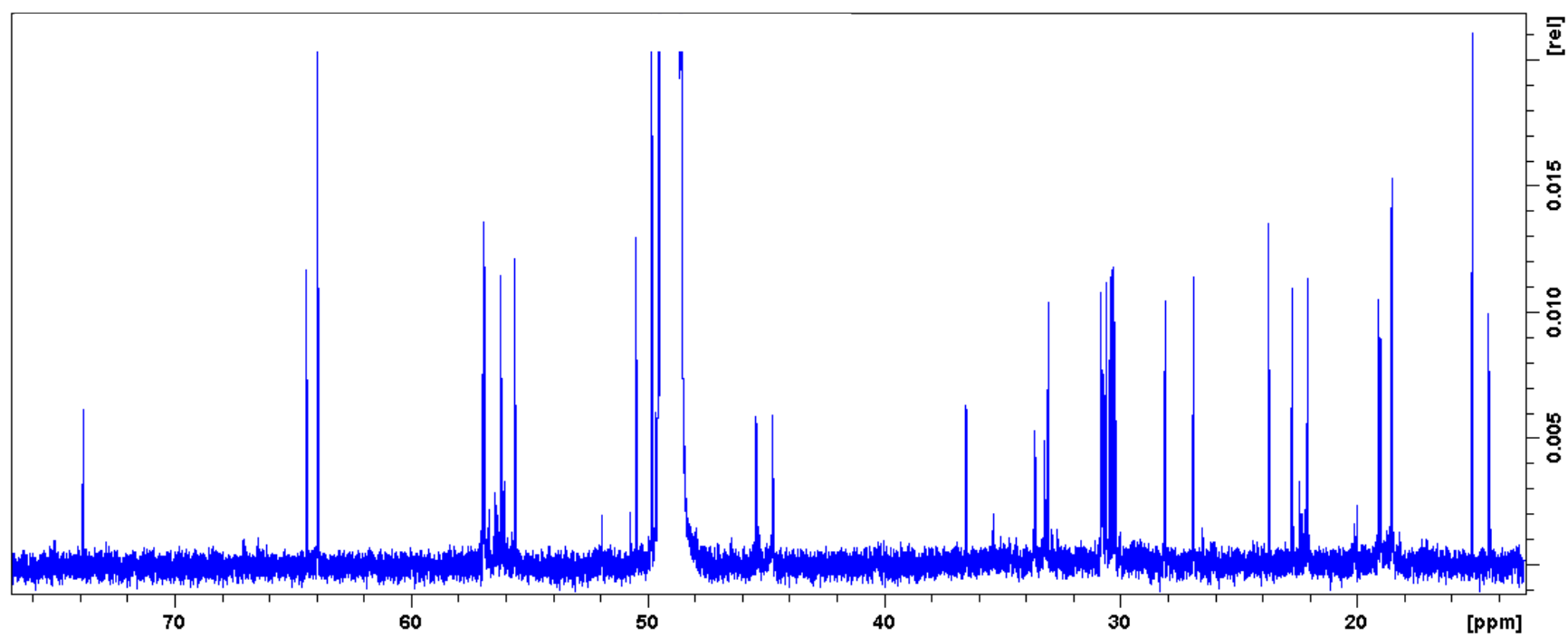


Figure S16c. ^{13}C spectrum of **2** from 75 to 15 ppm

Figures S17a-c. DEPT 135 NMR spectroscopic data of **2** in MeOD.

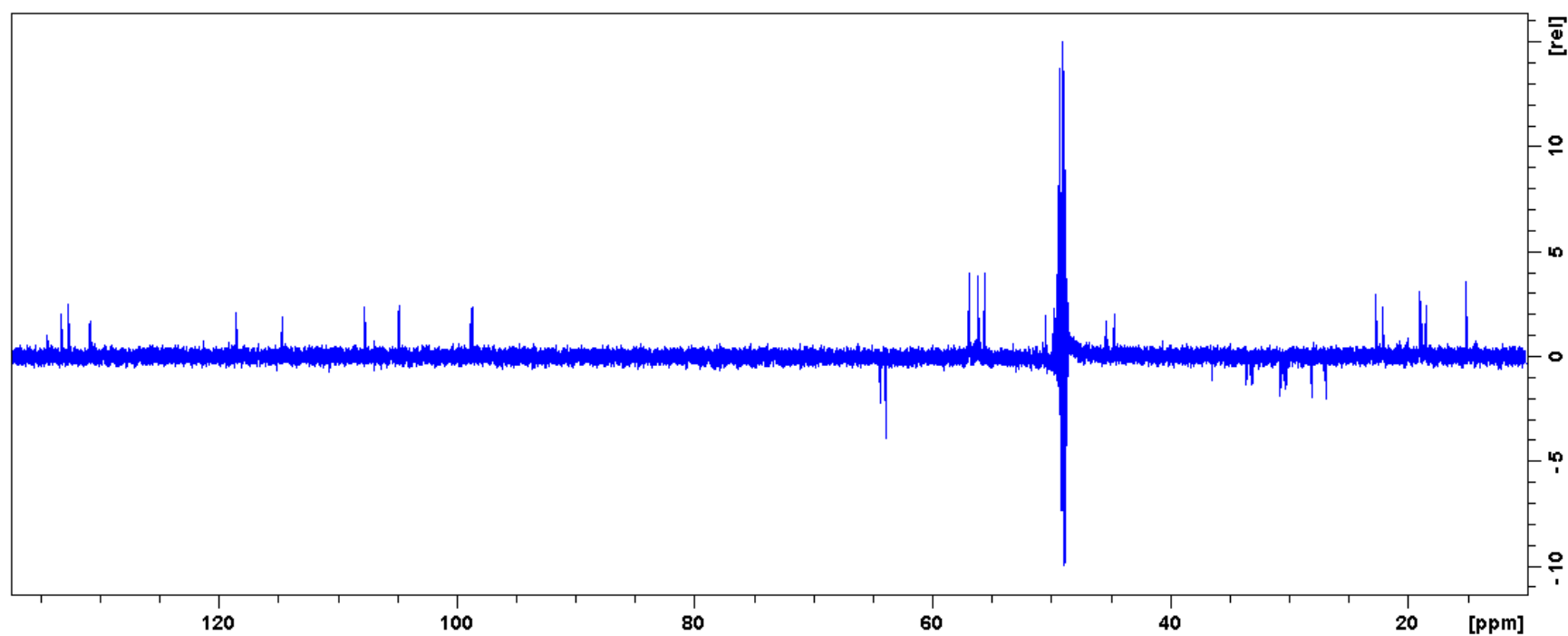
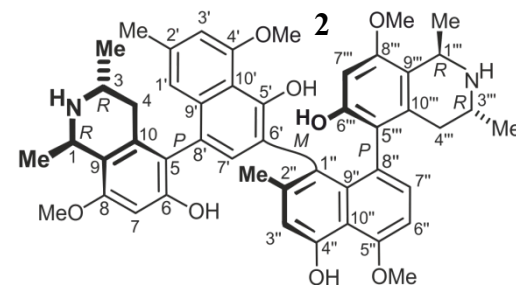


Figure S17a. Overall DEPT 135 spectrum of **2**

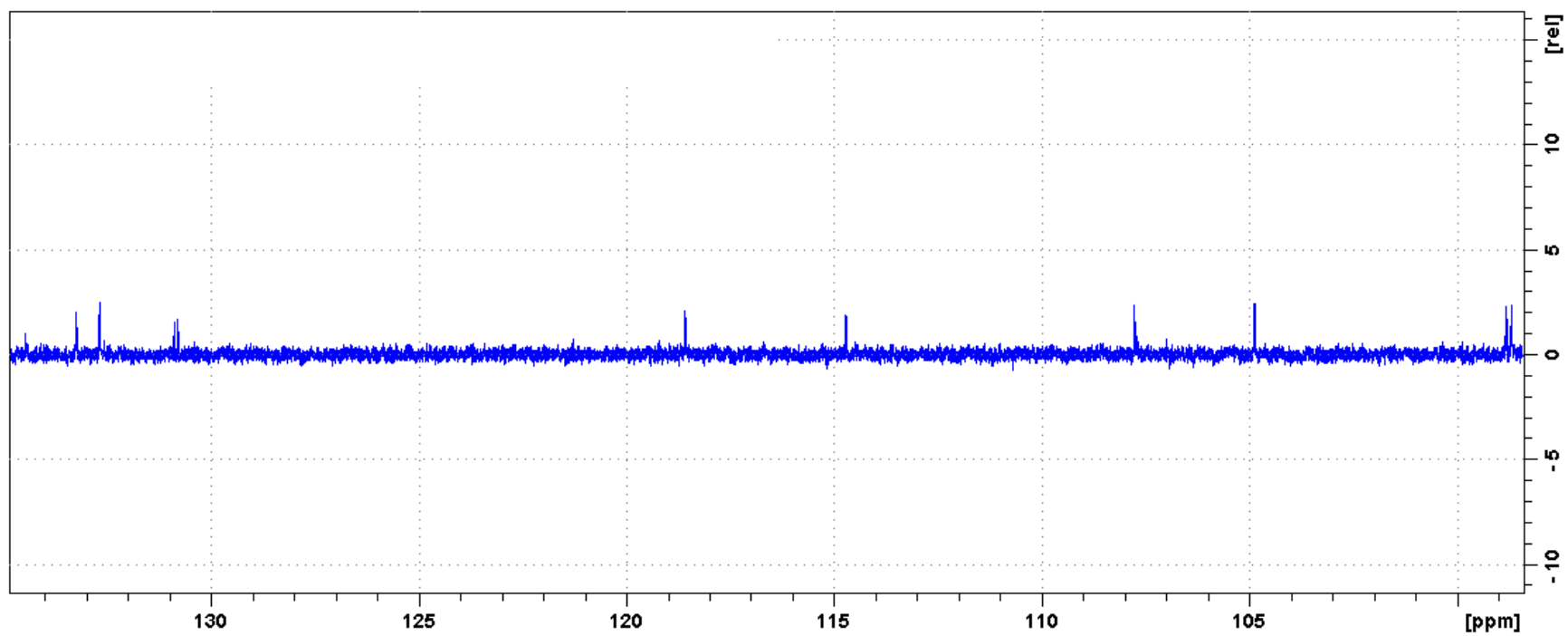


Figure S17b. DEPT 135 spectrum of **2** from 135 to 98 ppm

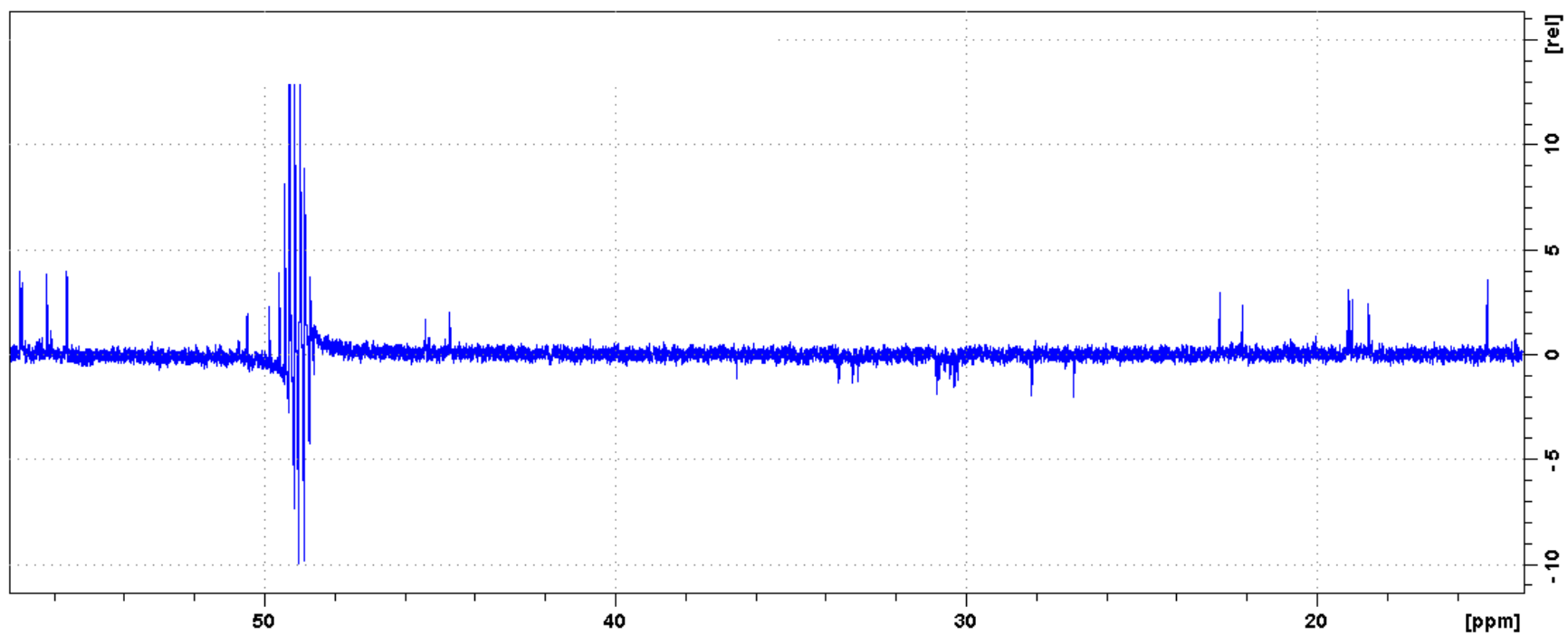


Figure S17c. DEPT 135 spectrum of **2** from 60 to 17 ppm

Figures S18a-c. COSY spectra of **2** in MeOD.

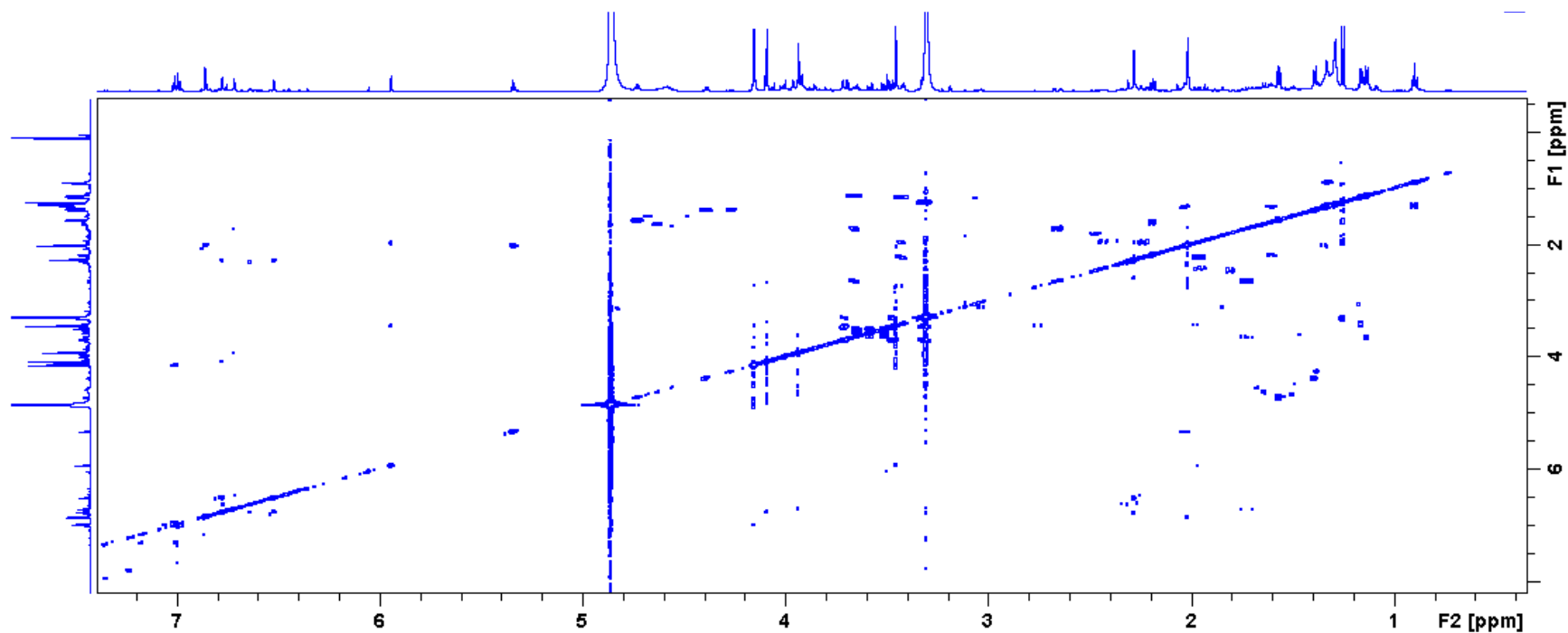
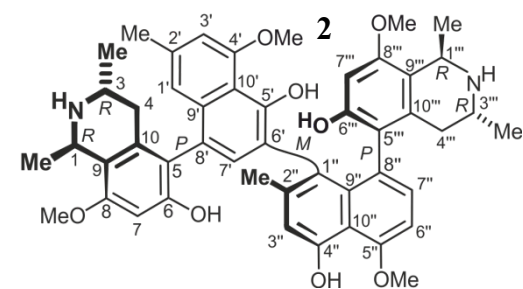


Figure S18a. Overall COSY spectrum of **2**

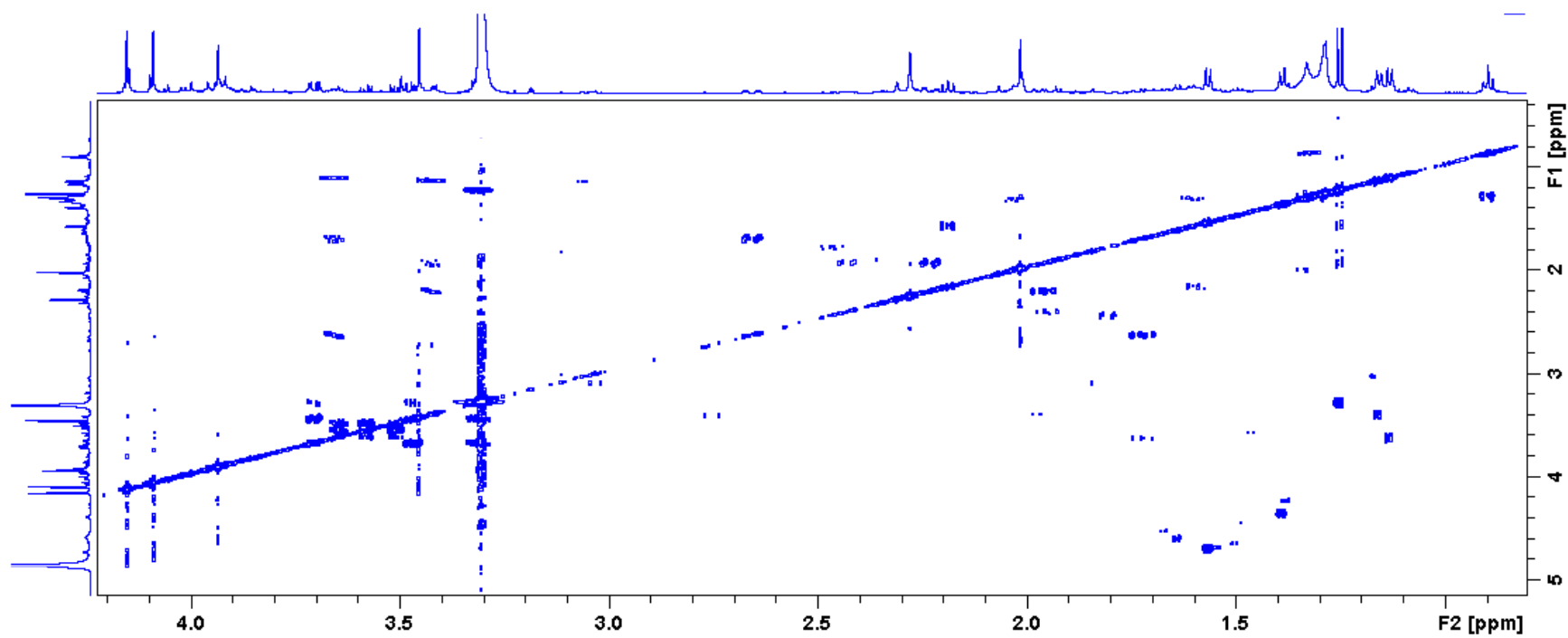


Figure S18c. COSY spectrum of **2** from 4.2 to 0.9 ppm

Figures S19a-c. ROESY spectra of **2** in MeOD.

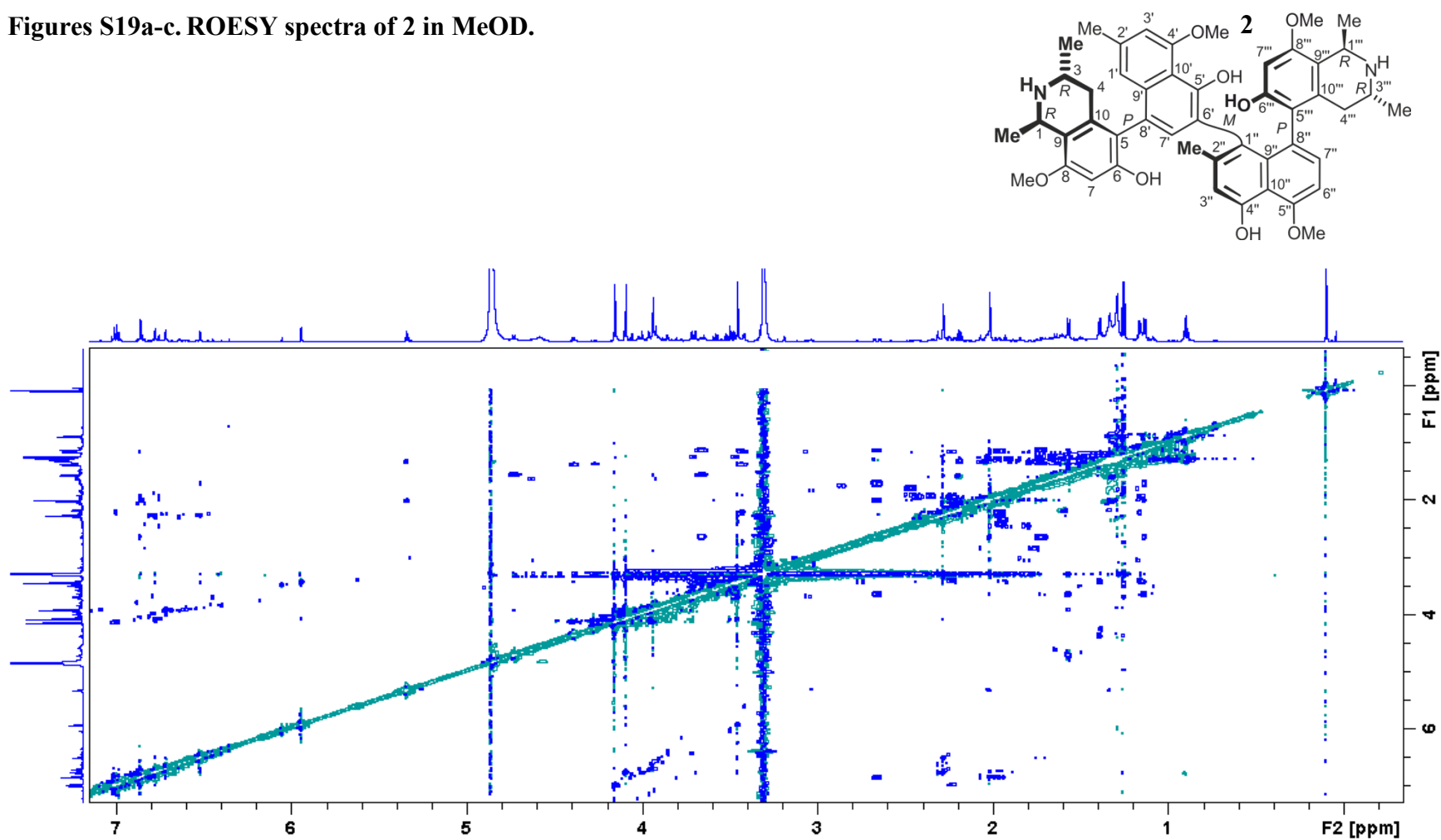


Figure S19a. Overall ROESY spectrum of **2**

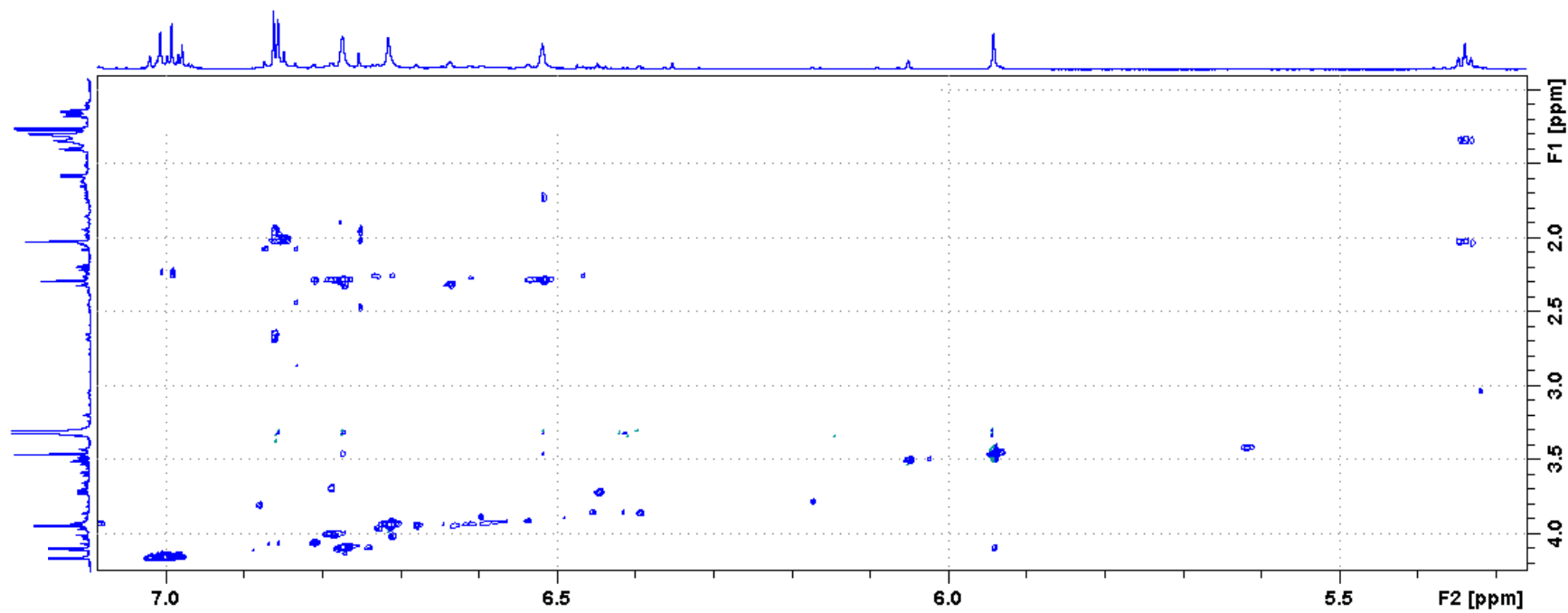


Figure S19b. ROESY spectrum of **2** from 7.1 to 4.3 ppm

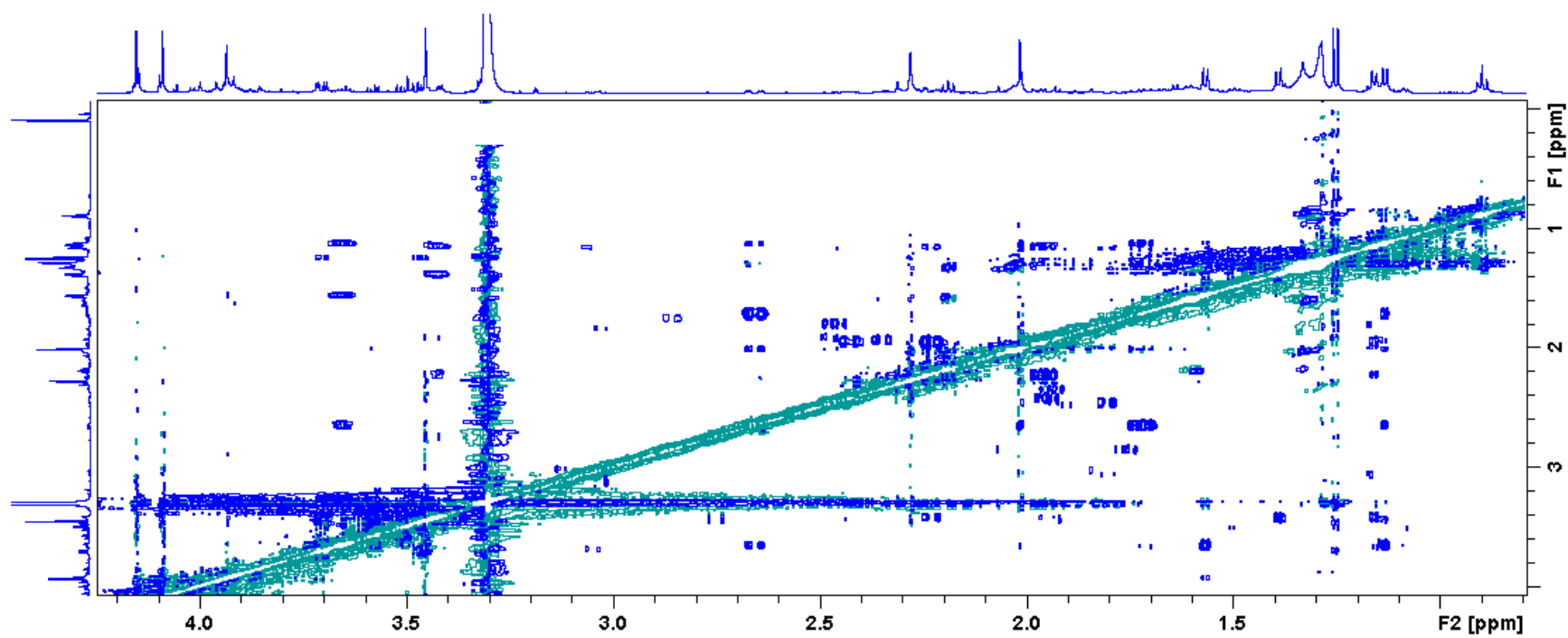


Figure S19c. ROESY spectrum of **2** from 4.2 to 0.9 ppm

Figures S20a-c. HSQC spectra of **2** in MeOD.

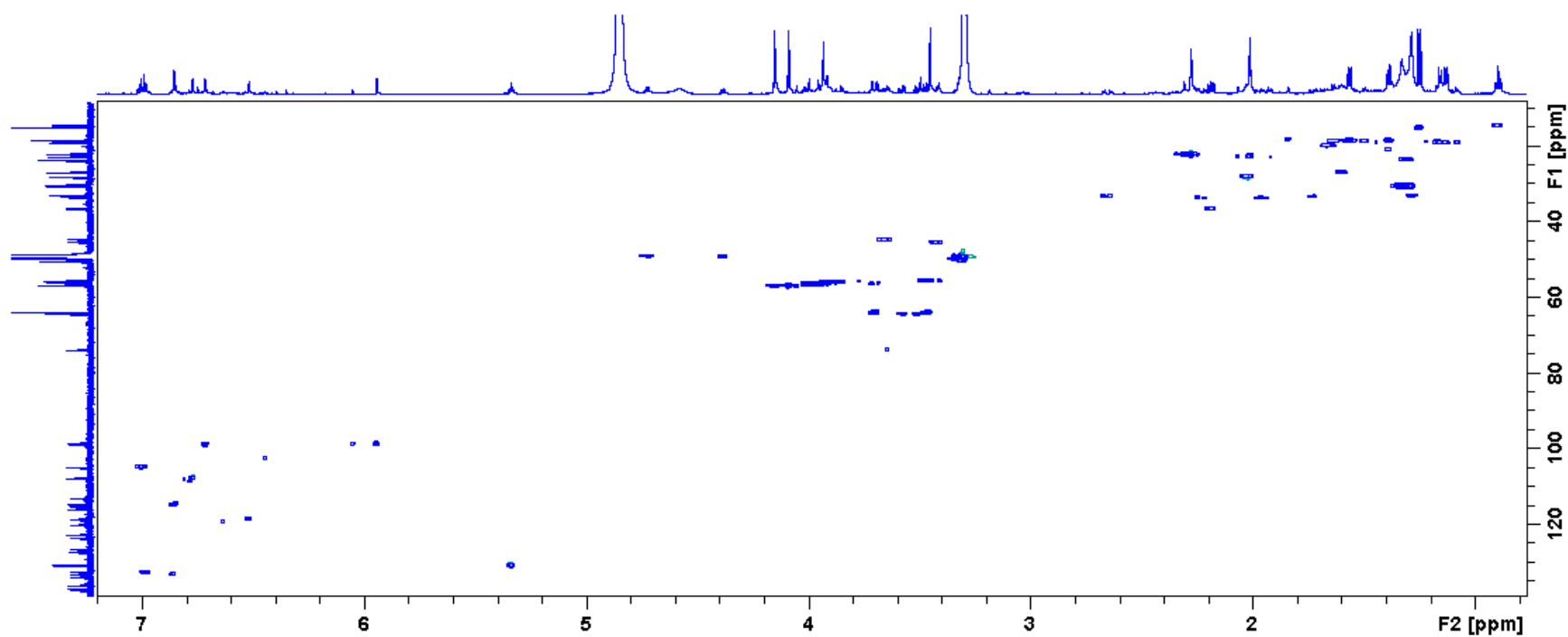
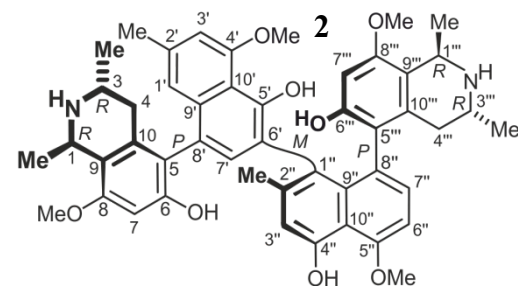


Figure S20a. Overall HSQC spectrum of **2**

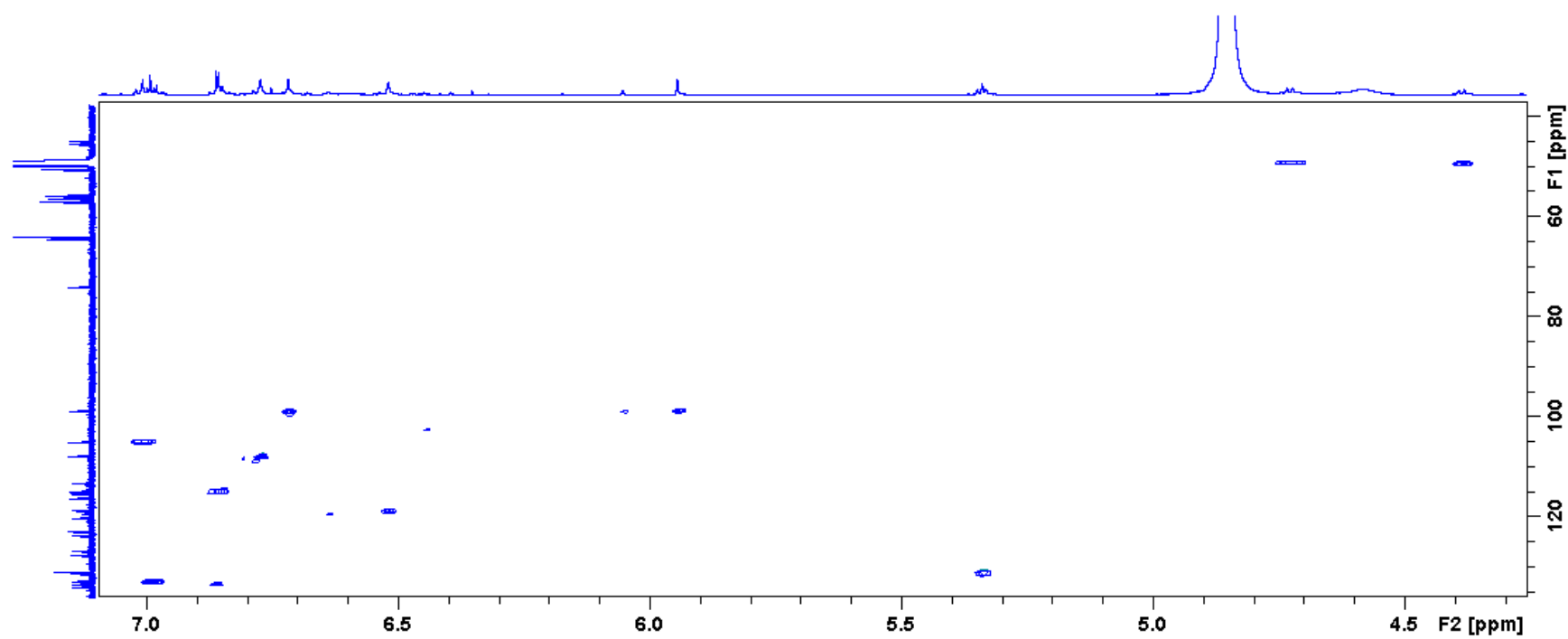


Figure S20b. HSQC spectrum of **2** from 7.1 to 4.3 ppm

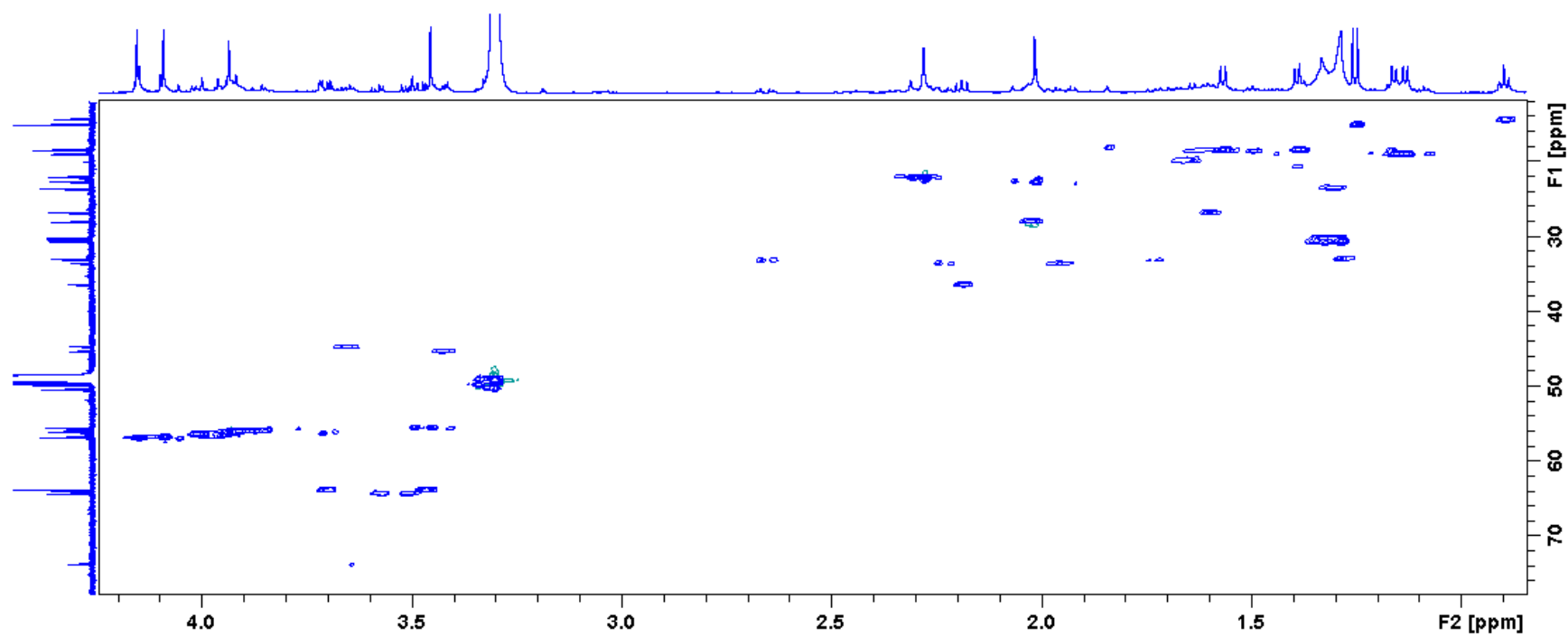


Figure S20c. HSQC spectrum of **2** from 4.2 to 0.9 ppm

Figures S21a-c. HMBC spectra of **2** in MeOD.

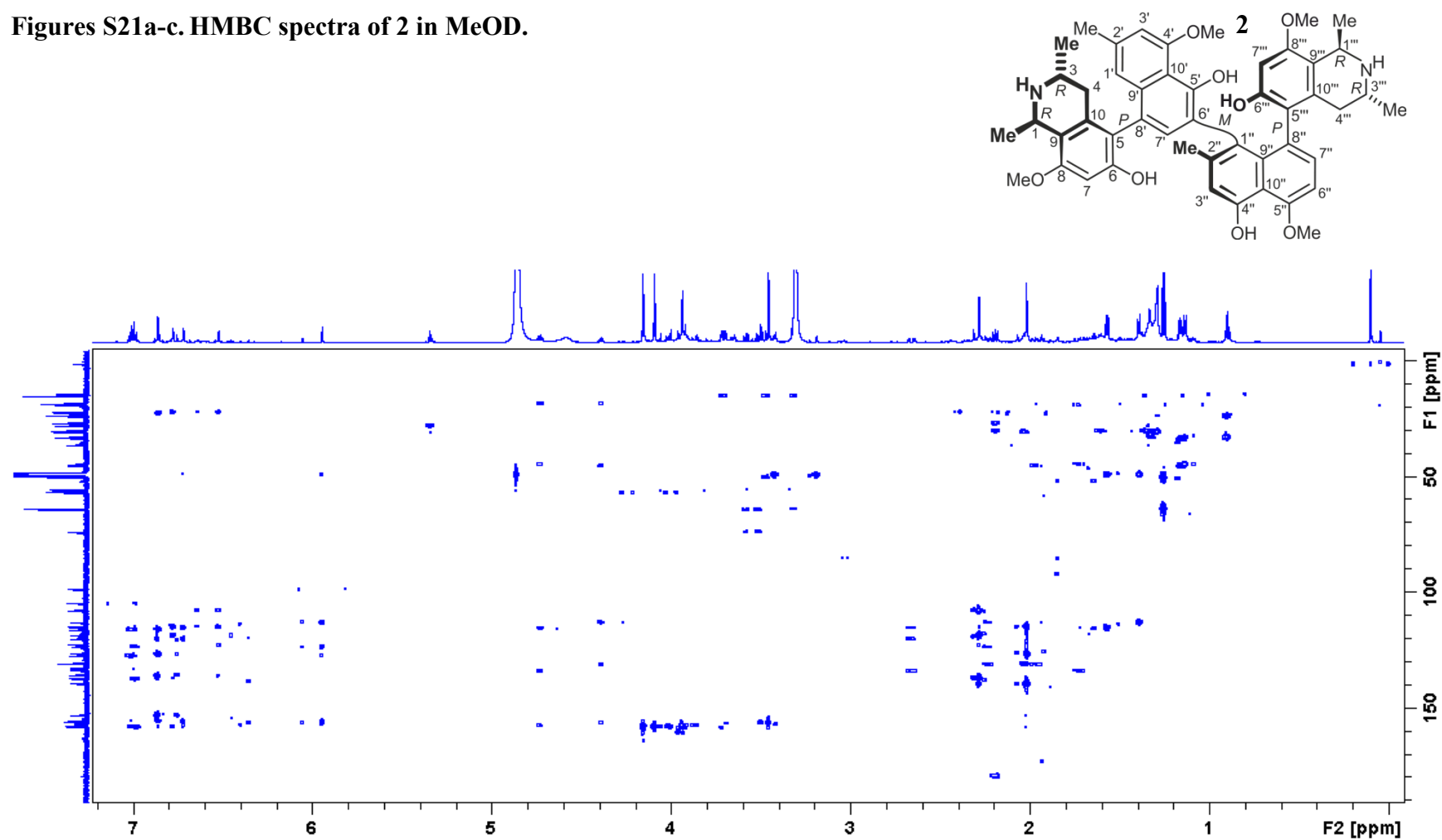


Figure S21a. Overall HMBC spectrum of **2**

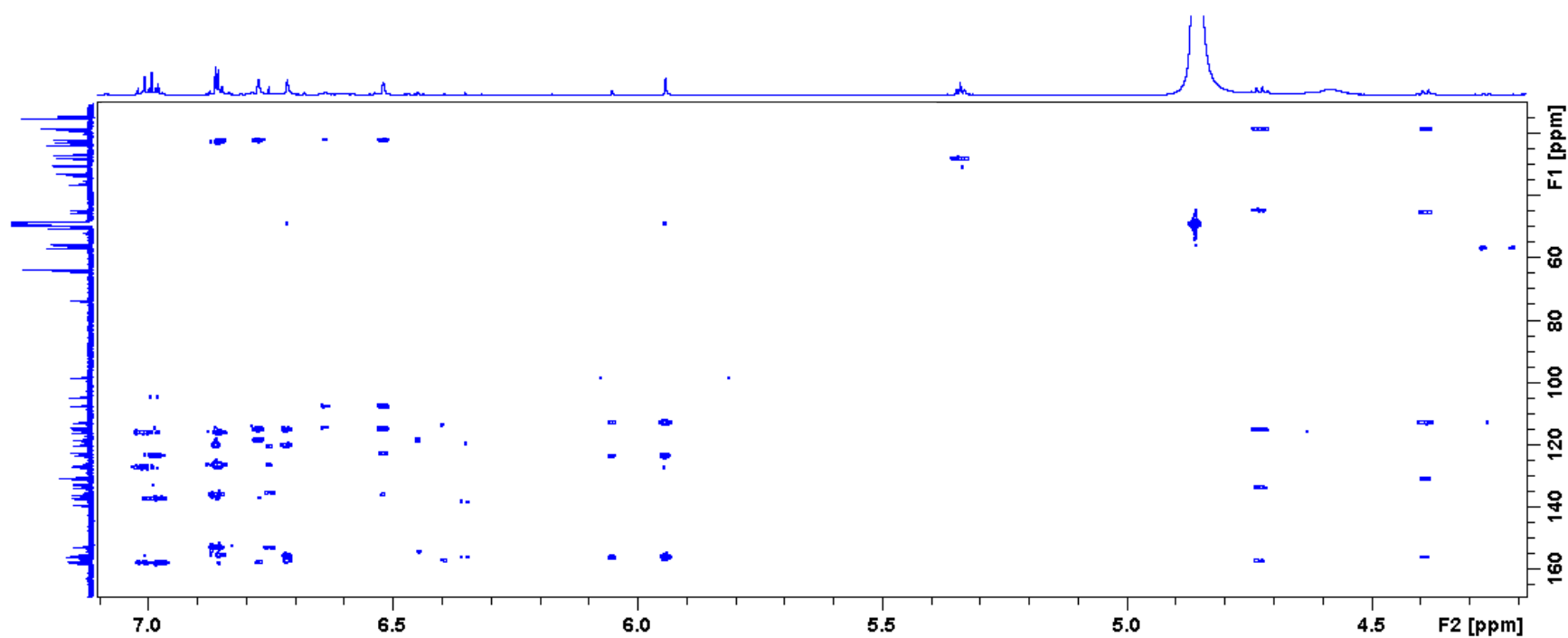


Figure S21b. HMBC spectrum of **2** from 7.1 to 4.2 ppm

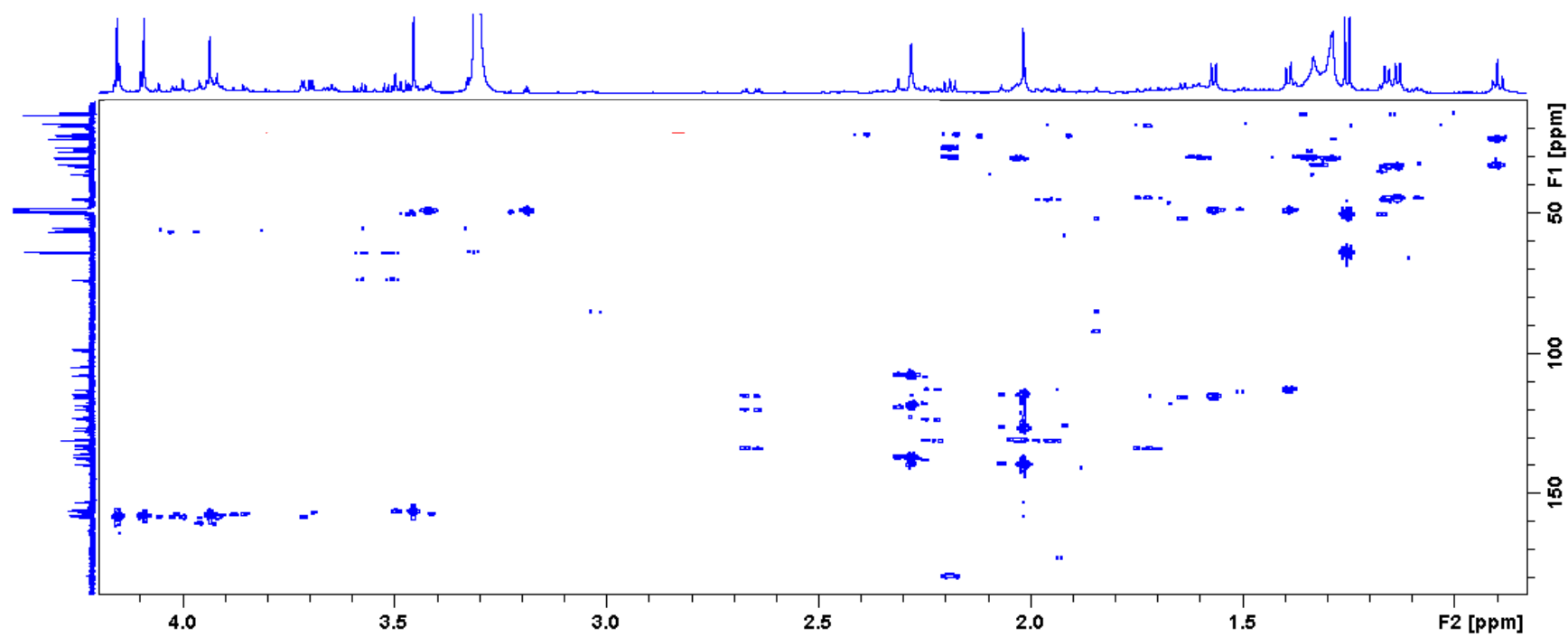
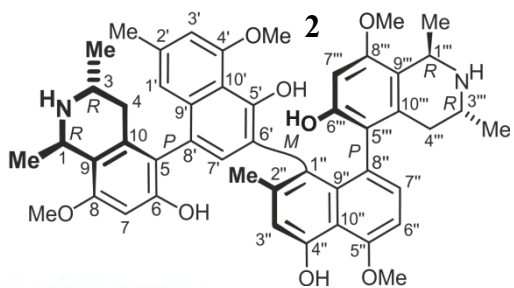


Figure S21c. HMBC spectrum of **2** from 4.2 to 0.9 ppm

Figure S22. HRESIMS spectrum of 2.



Acquisition Parameter

Source Type	ESI	Ion Polarity	Positive	Set Corrector Fill	49 V
Scan Range	n/a	Capillary Exit	150.0 V	Set Pulsar Pull	802 V
Scan Begin	50 m/z	Hexapole RF	400.0 V	Set Pulsar Push	804 V
Scan End	2800 m/z	Skimmer 1	50.0 V	Set Reflector	1700 V
		Hexapole 1	23.0 V	Set Flight Tube	8600 V
				Set Detector TOF	2000 V

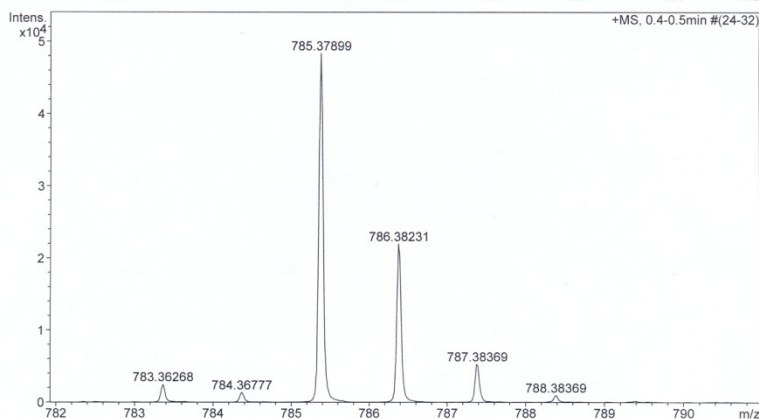
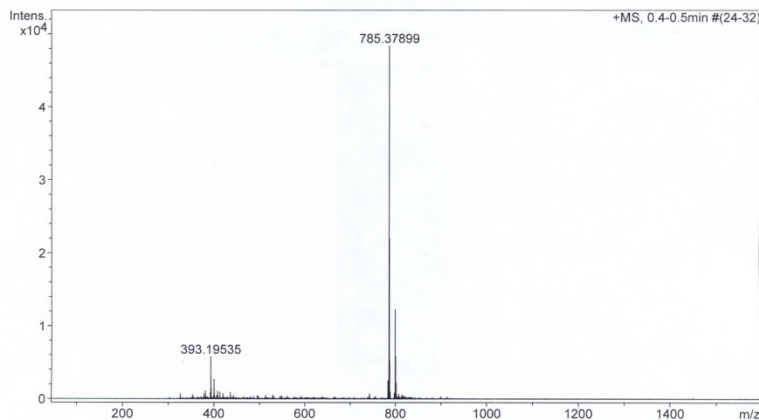


Figure S23. IR spectrum of 2.

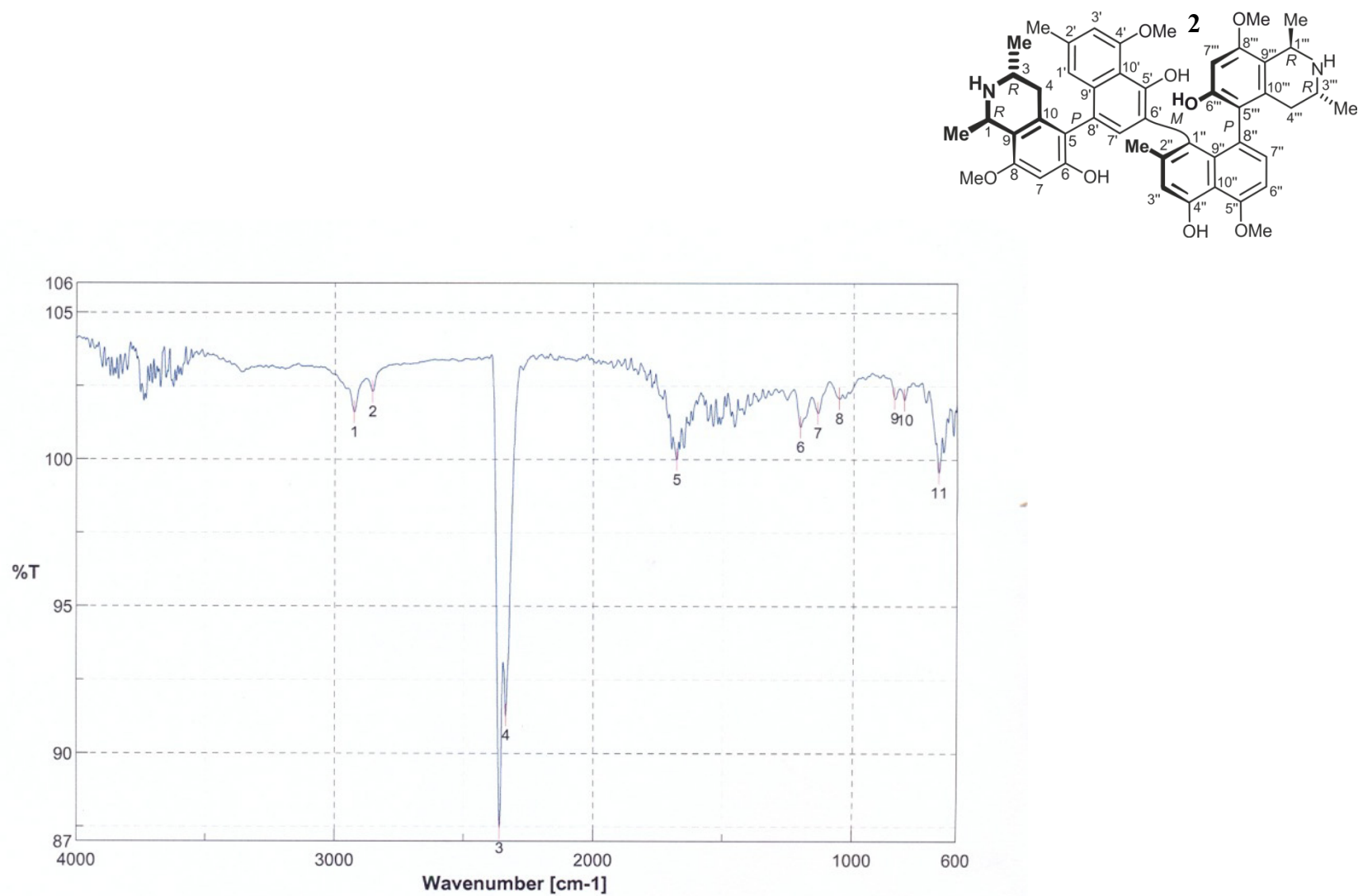


Figure S24. CD spectrum of 2.

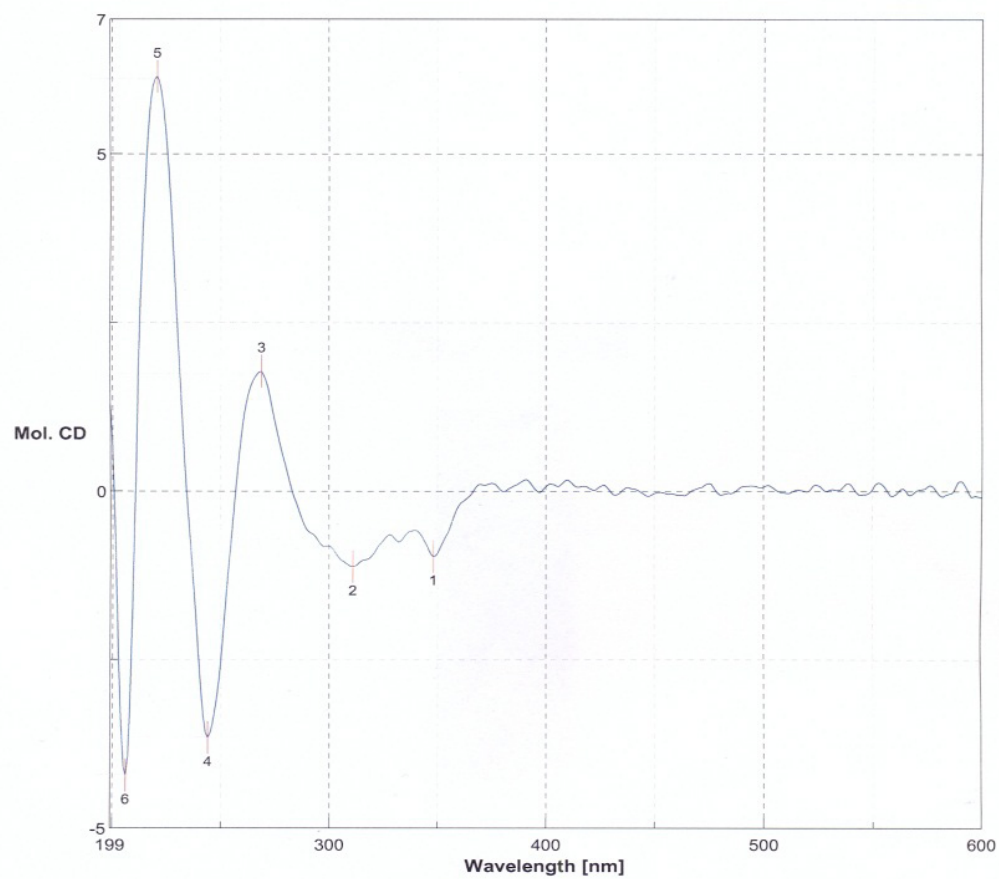
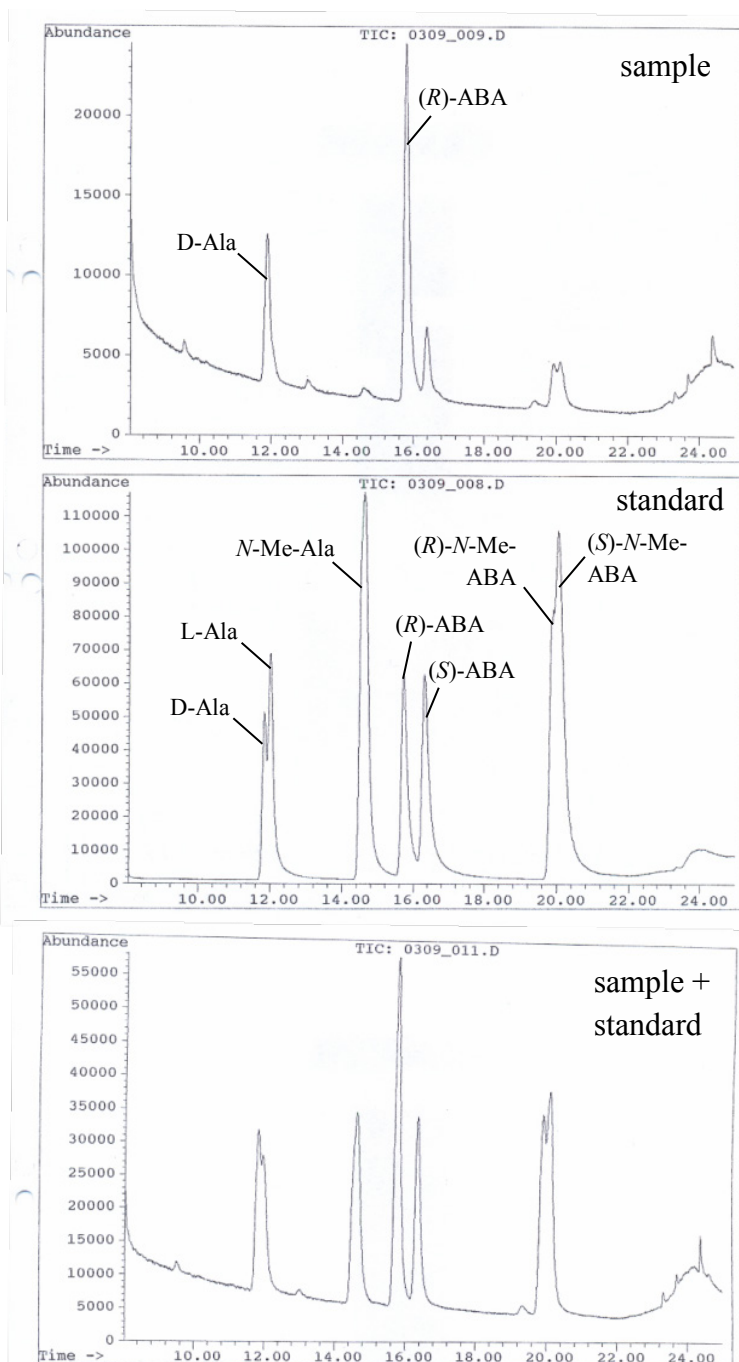
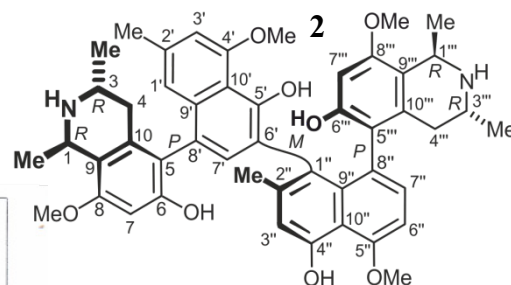


Figure S25. Oxidative degradation products of 2.



Ala = Alanine

N-Me-Ala = *N*-Methylalanine

ABA = 3-Aminobutyric acid

N-Me-ABA = *N*-Methyl-3-aminobutyric acid